2013

Flame Retardant Incorporation into Lithium-Ion Batteries

Ronald P. Dunn
University of Rhode Island, rdunn@chm.uri.edu

FLAME RETARDANT INCORPORATION INTO LITHIUM-ION BATTERIES

BY

RONALD P. DUNN

A DISSERTATION SUBMITTED IN PARTIAL FULFILLMENT OF THE

REQUIREMENTS FOR THE DEGREE OF DOCTOR OF PHILOSOPHY

IN

CHEMISTRY

UNIVERSITY OF RHODE ISLAND

2013

DOCTOR OF PHILOSOPHY DISSERTATION

Of

Ronald P. Dunn

APPROVED:

Dissertation Committee

Major Professor Dr. Brett L. Lucht

Dr. William B. Euler

Dr. David R. Heskett

URI: Dr. Nasser H. Zawia
Dean, The Graduate School - URI

UNIVERSITY OF RHODE ISLAND

2013

ABSTRACT

The use of Lithium-ion batteries (LIB's) in commercial electronics such as computers and cell phones has expanded in recent years. LIB technology offers higher energy density, lower self-discharge as well as higher operating voltage vs. other rechargeable battery technologies. However, the natural flammability of standard LIB carbonate based electrolyte along with risk of thermal runaway poses safety concerns. Thus, the research and development of nonflammable alternative electrolyte mixtures for standard LIB's is of high interest to researchers. To that end, Organophosphate containing Flame retardant (FR) compounds are being investigated as they possess natural fire suppressing qualities.

LIB utilization in large platform applications, such as electric vehicles (EV's) and aerospace designs has stimulated interest in higher energy density electrode materials such as Si. However, the practical use of Si does bring with it challenges related to the enormous volume changes which take place during cycling. The use of LIB's for large high energy applications raises elevated safety concerns relating to thermal runaway. Detailed investigations relating to the benefit, cycling performance, and effect on the solid electrolyte interphase (SEI) upon FR incorporation into LIB's with various anodes with/without SEI film stabilizing agents will be presented. SEI composition and structural changes upon FR incorporation are analyzed via surface analysis techniques including SEM and XPS.

ACKNOWLEDGMENTS

I would first like to thank my mentor Dr. Brett L. Lucht for his guidance, patience, and support during my research and training. It has been the utmost honor to have had the opportunity to learn from his knowledge and experience. I would also like thank Dr. Bill Euler for his constant support throughout my entire graduate school career as well as Dr. David Heskett, Dr. Sze Yang and Dr. Arijit Bose for reviewing my dissertation. I thank the University of Rhode Island for the opportunity to learn and to contribute to the scientific community. I would also like to thank Mr. Mike Platek at the University of Rhode Island – Department of Electrical Engineering for his guidance and assistance.

My deepest most special thanks go to the love of my life and my best friend, the most beautiful and most extraordinary girl in the cosmos, my wife Nancy for her relentless belief in me through the enormous challenges of my graduate school career. You light up my life every day and are always and forever the center of my universe.

I thank my dear friend Brandon Knight who has become family to me for being my wingman from day one. My friend, it has been a privilege. I thank my good friend Dr. Mengqing Xu for his friendship and constant support during my research. I thank all the member of the Lucht group past and present including Dr. Janak Kafle, Dr. Liu Zhou, Dr. Swapnil Dalavi, Dr. Dinesh Chalasani, Dr. Cao Nguyen, Dr. Rahul Kadam, Dr. Xiaobo Li, and Mike Lazar. I also thank Kyle Pereira and Dr. Chris Latendresse who I am honored to call my friends.

My awesome Dad who worked so hard to make sure I could pursue my dreams and who is the absolute best Dad in the history of the world. My greatest teacher, my Mom who taught me how to use the mind I was given, and for instilling in me the desire to always strive to excel and the pure love for learning. My incredible brother Kevin who is and always will be my hero and the best brother ever. My grandfather, grandmother, aunt, and also Mac and Marcia who I know have been and always will be watching over Nancy and I.

PREFACE

This dissertation is written in manuscript format. The first chapter provides an introduction to lithium-ion batteries, lithium-ion battery electrolyte and flame retardant cosolvents/additives. The second chapter is a manuscript published in the Journal of the Electrochemical Society. The third chapter is a manuscript that will be submitted to the Journal of Power Sources. The fourth chapter is a manuscript that will be submitted to the Journal of Power Sources.

TABLE OF CONTENTS

LIST OF TABLES

3. **Chapter 3**

4. **Chapter 4**

LIST OF FIGURES

1. **Chapter 1**

2. **Chapter 2**

4. **Chapter 4**

Chapter 1 – Introduction

Background

Lithium-ion batteries have fast become the preferred energy storage option for consumer electronics including laptop computers, and smartphones. In addition, Li-ion batteries are being utilized for large-scale applications such as hybrid and electric vehicles (EV's) as well as aerospace platforms. As compared to other battery systems such as NiZn, NiMH, and NiCd, Li-ion batteries offer lower self-discharge, superior operating voltage, wide operating temperature range, and higher gravimetric and volumetric energy density.[1,2]

The early use of Li metal anodes in rechargeable cells met with cell safety issues relating to Li dendrite accumulation on the surface of the Li during repeated cycling. The constant buildup of dendrites led to puncturing of the separator material and therein safety issues stemming from internal short circuit. The safety issues relating to use of Li metal as an anode led to the study of anode materials which allow for the reversible intercalation and deintercalation of Li ions. [2,3]

The current standard for Li-Ion batteries (Fig. 1) consists of a graphite anode on a Cu current collector together with a Li metal oxide cathode such as $LiCoO_2$, $LiNi_{0.8}Co_{0,2}O_2$ or $LiNi_{1/3}Co_{1/3}Mn_{1/3}O_2$ on an Al current collector. A polyolefin or polyethylene separator is utilized which provides electrical insulation between the terminals but allows for Li-ion migration during cycling.[1,2] Standard Li-Ion battery electrolyte uses either binary mixtures of ethylene carbonate (EC) combined with ethyl methyl carbonate (EMC) or ternary mixes of EC with diethyl carbonate (DEC) and

dimethyl carbonate (DMC) for a solvent along with Lithium hexafluorophosphate ($LiPF_6$) as the salt of choice.[2,4] The physical properties of these solvents are detailed in Table 1.[2,5] These mixtures are by their very nature flammable and thus the safety risks associated with thermal runaway pose concern.

Li-Ion battery Safety Issues

Li-Ion cell thermal runaway events can stem from any one of several causes including excessive heat buildup within cell, and/or cell overcharge/cell overdischarge. Internal short circuit via metallic dendrite accumulation as a result of poor manufacturing quality is also a trigger for a thermal runaway event. During an overcharge, significant heat within the cell leads to break down of the protective SEI (solid electrolyte interphase) film layer and separator material. The destruction of the SEI layer exposes the bulk electrode material now at states of extreme voltage and heat triggers conversion of the electrolyte into flammable gases. This over-delithiation of the cathode leads to failure of the cathode structure as well as the generation of oxygen and further heat evolution. Flammable gases build up also results in excess internal cell pressure. This process often leads to venting and subsequent ignition upon exposure to air as well as possible flame ignition inside the cell. Today, the majority Li-Ion cell models are fitted with safety relief valves/vents to reduce the possibility of explosion. However, the threat of thermal runaway upon individual Li-ion cells threatens fire spread to surrounding cells and therein the overall safety of the outside payload .[2,5,6]

Flame Retardant Incorporation

The possibility of thermal runaway poses significant safety threats most especially to large scale high power/energy applications such as electric and aerospace vehicles. These safety concerns have prompted researchers to investigate the feasibility of Flame retardant (FR) cosolvent/additive incorporation into standard Li-ion electrolyte. Organophosphate containing compounds are now being studied for their natural fire suppressing qualities.[5-7] Many research groups have reported using 4-Isopropyl Phenyl Diphenyl Phosphate (IPPP)[8], Diphenyloctyl phosphate (DPOF)[9], Triphenyl Phosphate (TPP) [10-14], and Dimethyl methylphosphonate (DMMP)[7,15-17] as FR cosolvents/additives for Li-Ion cells. The advantage through the use of these additives is to perfect a viable nonflammable alternative which offers comparable electrochemical performance to standard electrolyte mixtures. The origination of these flame mediating qualities is thought to stem via radical scavenging and therein halting of combustion or though char layer formation.[2,5-7] Chapter 2 of this dissertation discusses the FR benefits and electrochemical effects of the incorporation of Triphenyl phosphate (TPP) into Li-Ion batteries with standard Graphite anodes.

High Capacity Si Anodes

The higher energy and power requirements of large scale platforms such as electric automobiles and space vehicles have prompted the development of anodes with higher energy density. Si anodes are of keen interest as an anode material due to their significant theoretical specific capacity advantage (3579 mAh/g) vs. standard

Graphite anodes (372 mAh/g).[18] The practical use of Si anodes has been wrought with challenges relating to the immense volume variations (3-4 fold) that occur between their charged and discharged states resulting in substantial internal mechanical stresses. These physical stresses lead to loss of electrical contact between the Si anode active material and the Cu current collector. The surface variations of Si anodes during repeated cycling also leads to breakdown of the protective SEI and continual reformation. This continuous SEI formation results in large initial irreversible capacity loss, poor capacity stability and over the long term shorter cell life.[18,19]

Many research groups have been investigated thin-film Si anodes as well as Si-inactive composite materials with decreased Si particle size and alternative binder. [20-23] These efforts are directed towards mediation of the enormous mechanical strains associated with repeated cycling of Si anodes. The cycling benefits offered via the use of SEI film stabilizing additives such as lithium bis(oxalato)borate (LiBOB) and fluoroethylene carbonate (FEC) have also been explored by various groups.[24-26] Chapter 3 of this dissertation describes the electrochemical effects of Triphenyl phosphate (TPP) and Dimethyl methyl phosphonate (DMMP) FR cosolvent incorporation into Li-Ion batteries with Thin-film Si anodes. Chapter 4 of this dissertation covers the incorporation of TPP and DMMP into Li-Ion batteries with Si nanoparticle anodes.

References

1. D. Linden., Handbook of Batteries, fourth ed., McGraw-Hill Professional, New York, 2010.

2. K. Xu, Chem. Rev. 104 (2004) 4303.

3. J.R. Dahn, Phys. Rev. B: Condens.Matter, 44, (1991), 9170.

4. M. C. Smart, B. V. Ratnakumar, S. Surampudi, J. Electrochem. Soc. 146 (1999) 486-492.

5. G. Nagasubramanian, K. Fenton, J. Power Sources. 101 (2013) 3-10.

6. K. Xu, M. S. Ding, S. Zhang, J. L. Allen, T. R. Jow, J. Electrochem. Soc. 149 (2002) A622-A628.

7. S. Dalavi, B.L.Lucht, B. Ravdel, M. Xu, L.Zhou, J. Electrochem. Soc. 157, (2010) A1113-A1120.

8. Q.Wang, J. Sun, X.Yao, C. Chen, Electromchem, Solid State Lett. 8 (9) (2005) A467-A470.

9. E. G. Shim, T. H. Nam, J. G. Kim, H. S. Kim, and S. I. Moon, Electrochimica Acta. 54, (2009) 2276-2283.

10. E. G. Shim, T. H. Nam, J. G. Kim, H. S. Kim, and S. I. Moon, J. Power Sources.172 (2007) 919-924.

11. K. A. Smith, M. C. Smart, G. K. S. Prakash, and B. V. Ratnakumar, ECS Trans. 16(35) (2009) 33-41.

12. M. C. Smart, F. C. Krause, C. Hwang, W. C. West, J. Soler, G. K. S. Prakash, and

B. V. Ratnakumar, ECS Trans. **35**(13) (2011) 1-11.

13. E. G. Shim, T. H. Nam, J. G. Kim, H. S. Kim, S. I. Moon, J. Power Sources, 172 (2007) 901-907.

14. Y. E. Hyung, D. R. Vissers, and K. Amine, J. Power Sources, 119-121 (2003) 383-387.

15. H. F. Xiang, Q. Y. Jin, C. H. Chen, X. W. Ge, S. Guo, J. H. Sun, J Power Sources,174 (2007) 335-341.

16. H. F. Xiang, H. Y. Xu, Z. Z. Wang, C. H. Chen, J. Power Sources, 173 (2007) 562-564.

17. J. K. Feng, X. P. Ai, Y. L. Cao, H. X. Yang, J. Power Sources, 177 (2008) 194-198.

18. U. Kasavajjula, C. Wang, A.J. Appleby, J. Power Sources 163 (2007) 1003.

19. S.P.V. Nadimpalli., V.A. Sethuraman., S. Dalavi., B.L. Lucht., M.J. Chon., V.B. Shenoy., P.R. Guduru, J. Power Sources. 215, (2012) 145-151.

20 S. Dalavi, P.R. Guduru, B.L. Lucht, J. Electrochem. Soc. 159 (2012) A642.

21. W.R. Liu, Z.Z Guo, W.S.Young, D.T. Shieh, H.C.Wu, M.H. Yang, N.L. Wu, J. Power Sources, 140 (2005) 139-144.

22. A.Magasinski, B. Zdyrko, I. Kovalenko, B. Hertzberg, R. Burtovyy, C. F. Huebner, T. F. Fuller, I. Luzinov, and G. Yushin, ACS Applied Materials & Interfaces 2 (11) (2010) 3004-3010.

23. H. Buqa, M. Holzapfel, F. Krumeich, C. Veit, P. Novak, J. Power

24. N. Choi, K. Yew, H. Kim, S. Kim,W. Choi, J. Power Sources, 172 (2007) 404-409.

25. V. Etacheri, O. Haik, Y. Goffer, G.A. Roberts, I.C. Stefan, R. Fasching, D. Aurbach, Langmuir 28 (2012) 965.

26. H. Nakai, T. Kubota, A. Kita, A. Kawashima, J. Electrochem. Soc., 158, (2011) A798-A801.

	MW	Structure	Mp (°C)	Bp (°C)	Dielectric Constant (25°C)	Viscosity (25°C)	Flash Point (°C) Closed Cup
EC	88	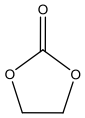	36.4	248	89.78	1.90 @ 40°C	145
EMC	104	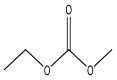	-53	110	2.958	0.65	23
DMC	90	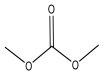	4.6	91	3.107	0.59	18
DEC	118	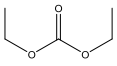	-74.3	126	2.805	0.75	33

Table 1-1**.** Properties of Std. Li-Ion battery electrolyte components.

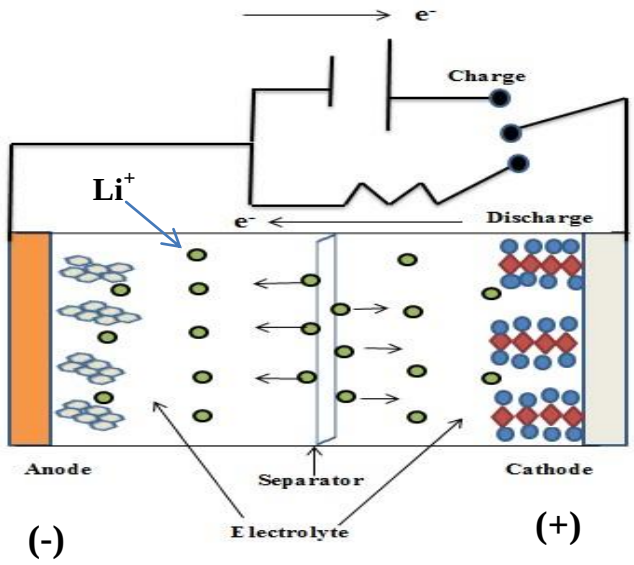

Fig.1-1. Standard Li-Ion Battery Concept

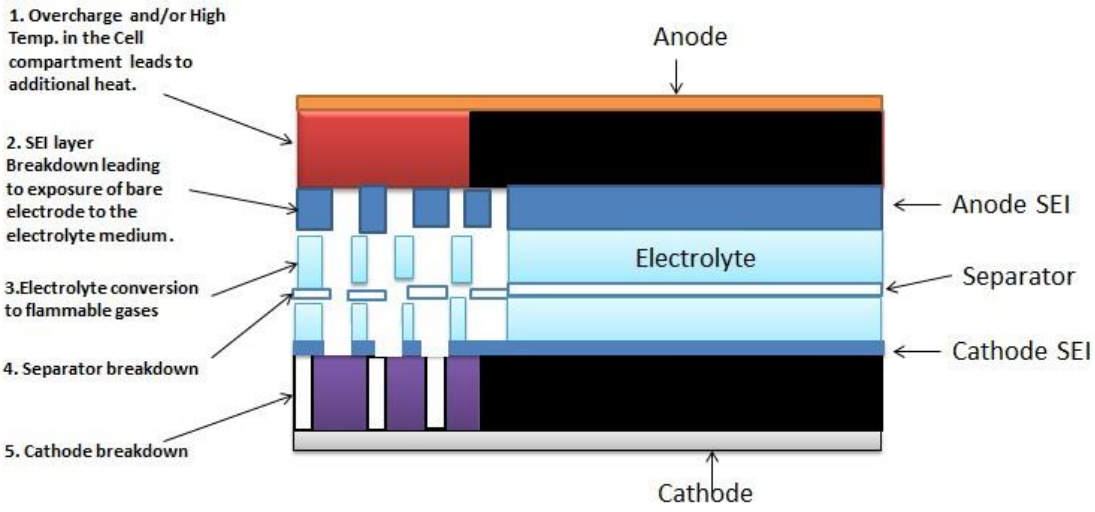

Fig. 1-2. Thermal Runaway

Chapter 2

Electrochemical Analysis of Li-Ion Cells Containing Triphenyl Phosphate

Ronald P. Dunn,[1] Janak Kafle,[1] Frederick C. Krause,[2] Constanza Hwang,[2] Bugga V. Ratnakumar,[2] Marshall C. Smart,[2] and Brett L. Lucht[1]

[1]*Department of Chemistry, University of Rhode Island,*

Kingston, Rhode Island 02881, USA

[2]*Jet Propulsion Laboratory, California Institute of Technology,*

4800 Oak Grove Drive, Pasadena, CA 91109

The following was published in the *Journal of the Electrochemical Society*, and is presented here in manuscript format.

Abstract

The development and subsequent incorporation of flame retardant additives (FRAs) has become a priority for Li-Ion battery research and development. Triphenyl phosphate (TPP) was studied to ascertain the safety benefits and electrochemical performance when incorporated into a $LiPF_6$/ethylene carbonate (EC)/ethyl methyl carbonate (EMC) electrolyte system. The flammability of electrolytes containing TPP was investigated via self-extinguishing time and flash point analysis. The electrochemical stability was studied by cyclic voltammetry (CV), battery cycling in graphite/$LiNi_{0.8}Co_{0.2}O_2$ cells, electrochemical impedance spectroscopy (EIS) and Tafel polarization. In order to better understand the role of TPP, ex-situ surface analysis of the cycled electrodes was conducted with X-ray photoelectron spectroscopy (XPS) and scanning electron microscopy (SEM). Incorporation of TPP results in a moderate decrease in the flammability of the electrolyte with relatively minor detrimental effects on the performance of the cells and thus is a promising additive for lithium ion batteries.

Introduction

Lithium-ion battery technology in recent years has proven itself as a dependable energy storage medium for commercial consumer electronics. Li-ion batteries offer higher operating cell voltage, higher energy density, longer cycle life and lower self-discharge. These advantages make Li-ion cells superior to other rechargeable systems such as Ni-MH and Ni-Cd. Safety issues however remain a concern with today's Li-ion batteries since the electrolyte is typically a blend of ethylene carbonate (EC) with

ethyl methyl carbonate (EMC) with a lithium salt, such as lithium hexafluorophosphate ($LiPF_6$). These electrolyte solutions are flammable and a risk of thermal runaway is a concern. The main causes of Li-ion cell thermal runaway are attributed to both internal short via metallic dendrite accumulation and/or cell overcharge leading to destabilizing over-deliathiation of the cathode.[1-5]

The potential for thermal runaway has led to efforts to reduce the fire risk and the propagation within Li-ion cells. Many of these efforts focus on the development, and subsequent incorporation, of flame retardant additives (FRA) into the electrolyte solution. A number of organophosphorus compounds have been investigated for lithium ion batteries. For example, various research groups have reported the use of trimethyl phosphate (TMP),[6] triphenyl phosphate (TPP)[3,7-11], tris(2,2,2-trifluoroethyl) phosphate[12-14], and dimethyl methylphosphonate (DMMP)[1,4,15] in lithium ion battery electrolytes. These additives are believed to result in lower electrolyte flammability due to the formation of a layer of char which protects the uncombusted condensed phase and/or the decomposition products serving as radical scavengers in the gas phase inhibiting combustion chain reactions.[16,17] Of the phosphate-based FRAs, triphenyl phosphate (TPP) is especially attractive since it has been reported to improve the safety of Li-ion cells under abuse conditions by lowering the flammability of electrolytes when incorporated in sufficient proportion[18], and it has been observed to provide good life characteristics[7,9].

Some FRAs have been observed to disrupt the formation and stability of the anode solid electrolyte interphase (SEI) layer, and are thus detrimental to the cycling performance of the cells. FRAs have also been investigated in combination with SEI

forming additives such as lithium bis(oxalato)borate (LiBOB) or vinylene carbonate (VC) which generate a more stable anode SEI and limit the detrimental effects of the FRA.[7,9,19] A stable SEI layer is critical to the proper functioning of Li-Ion cells, allowing the intercalation and de-intercalation of Li^+ at the graphite anode and preventing further reduction of the electrolyte.[2] The formation mechanisms of the SEI and the role of the constituent solvents and salts in the solid electrolyte interphase (SEI) are currently under investigation.[20]

This current research is focused upon the effort to inhibit flammability of electrolytes via incorporation of FR additives while mitigating their negative attributes and maximizing electrochemical performance. The drawbacks of FRA incorporation into lithium-ion batteries include increased discharge capacity fade and poor cycling performance at low temperatures. Loss of electrochemical performance in the presence of FR additives is commonly attributed to inadequate formation of a stable SEI on the surface of the anode, and in some cases undesirable properties of the cathode electrolyte interphase (CEI).[21,22] This investigation focuses on the effects of the incorporation of TPP on the flammability of the electrolyte, the conductivity of the electrolyte, the cycling performance of graphite/$LiNi_{0.8}Co_{0.2}O_2$ cells, electrode transfer kinetics, and electrode interphase structure in lithium ion batteries.

Experimental

Battery-grade carbonate solvents ethylene carbonate (EC), ethyl methyl carbonate (EMC), and dimethyl carbonate (DMC), as well as lithium

hexafluorophosphate ($LiPF_6$) salt, were obtained from Novolyte Technologies, Inc. Two different electrolytes 1.2 M $LiPF_6$ in EC/EMC (3:7 vol.%, BL1) and 1.0 M $LiPF_6$ in EC/EMC (2:8 vol.%, BL2) were obtained from Novolyte Technologies and utilized without further purification (water content was less than 50 ppm in all cases). Triphenyl phosphate (TPP) was obtained from Thermo Fisher Scientific at 99% purity and used as received. TPP containing electrolytes were prepared with a constant concentration of $LiPF_6$ and EC while EMC was replaced with TPP.

Self-extinguishing time, or SET, of the electrolyte combinations was measured via a modified version of the procedure detailed by Xu and coworkers using commercial cotton swabs as the test wick.[1,12] The commercial cotton swab wicks were manufactured to a uniform diameter of 1 cm and were injected with 100 µl of electrolyte. The wick was placed in a fume hood with an air flow velocity of 90 ft/s and suspended at uniform height above a watch glass. Burning time was recorded with the use of a digital stopwatch. This procedure was performed on ten samples of each electrolyte and an average SET was calculated for each.

The flash points of solvent blends incorporating TPP were measured using a Pensky-Martens Closed Cup Flash Tester from Koehler Instrument Company. Solvent blends were mixed excluding Li salt to a total mass of 70 g and placed in a closed test cup. A motorized stirrer was used to enhance solvent evaporation within the closed cup and a propane supplied flame was dipped into the sample cup every 1°C to test for vapor ignition signaling the flash point of the sample.

Conductivity measurements were performed with a Thermo Scientific Orion 3 Star conductivity benchtop meter using an Orion 011050MD 2-electrode conductivity probe (the cell constant value was 0.976 cm^{-1}). The probe was sealed under Ar in a threaded Ace glass cell and threaded Teflon adapter and O ring to avoid moisture contamination of the electrolyte. The cell was filled with approximately 9 mL of electrolyte solution and the cell was placed in a Tenney environmental chamber. Conductivity readings were recorded after 4 hour equilibration time between -60°C to 30°C.

Cyclic voltammetry (CV) was utilized to establish the electrochemical window of the electrolyte on the anode. Lithium metal was utilized as a reference and counter electrode, while a glassy carbon electrode was used as the working electrode. Three reduction potential sweeps were performed between 0 V and 3.0 V versus Li/Li^+ at a scan rate of 0.01 V/s. All experiments were carried out using a VersaSTAT 3-200 with FAR option Electrochemical WorkStation (Princeton Applied Research).[1]

Coin cells were assembled utilizing electrodes obtained from Yardney Technical Products. The anodes were composed of 89% mesocarbon microbead (MCMB), 8% poly(vinylidene difluoride) (PVDF) binder, and 3% conductive carbonaceous dilutant on a copper foil current collector. Cathodes contained 89% $LiNi_{0.8}Co_{0.2}O_2$, 5% PVDF and 6% conductive carbonaceous dilutant on an aluminum foil current collector. Preparation of the electrolyte and coin cell assembly was performed in a pure Argon atmosphere glove box with a water content < 5 ppm. Cells were constructed and cycled between 4.1 V and 3.0 V using an Arbin BT4010 battery cycler at 60 °F (15.5 °C).

The cycling protocol followed an initial formation cycling schedule with the first cycle at a C/20 current rate, followed by C/10 during cycles two and three, and C/5 for cycles four and five. Nominal cycling was conducted at C/5 current rate for an additional 30 cycles. The cells were then opened in an Ar filled glove box after a total of 35 cycles. Electrodes were extracted and rinsed three times with dimethyl carbonate (DMC) to remove residual salts. The rinsed electrodes were then vacuum dried overnight prior to surface film and morphological examination.

Larger experimental three-electrode cylindrical cells (approximately 400 mAh in capacity) were also assembled, which consisted of O-ring sealed, glass cells containing anodes (89% mesocarbon microbead (MCMB), 8% poly(vinylidene difluoride) (PVDF) binder, and 3% conductive carbonaceous dilutant on a copper foil current collector), cathodes (89% $LiNi_{0.8}Co_{0.2}O_2$, 5% PVDF and 6% conductive carbonaceous dilutant on an aluminum foil current collector), and lithium reference electrodes separated by two layers of polyethylene (Tonen-Setella) separator material. The anodes were coated with active material on both sides of the substrate and had an active material area of approximately 158 cm^2, corresponding to an electrode loading of 16 mg/cm^2. The NCO electrodes were also coated on each side with an active material area of approximately 141 cm^2, corresponding to a loading of 19 mg/cm^2.

Electrochemical characterization, including linear micro-polarization and Tafel polarization measurements, were performed using an EG&G potentiostat/galvanostat (273A) interfaced with a computer using Softcorr 352 software. To perform electrochemical impedance spectroscopy (EIS) measurements, a Solartron 1255 frequency response analyzer was used in conjunction with this potentiostat. All cells

were fully charged prior to impedance measurements, with the open circuit voltage > 4.07 V. Charge-discharge measurement and cycling tests were performed utilizing an Arbin battery cycler. The formation cycling was performed at current densities of 0.25 mA/cm2 (~C/16 rate) and the cells were charged to 4.10 V, followed by a tapered charge period at constant potential until the current decayed to a C/100 rate, and discharged to 2.75 V. For low temperature discharge rate characterization, the cells were charged at room temperature and allowed to soak at the desired temperature (in a Tenney environmental chamber with temperature control of +/- 1^{o}C) for at least five hours prior to discharging to 2.00 V.

Surface species characterization was accomplished via the collection of X-ray photoelectron spectroscopy (XPS) spectra using a PHI 5500 system and Al Kα radiation. A graphite reference peak of 284.3 eV was used for proper final shifting of the spectra collected. Multipak versions 6.1 as well as XPS Peak 4.1 software were utilized for analysis and curve fitting of collected spectra respectively. A combination of Gaussian and Lorentzian functions was used for the least squares curve fitting. The surface morphology of cycled electrodes was examined using a JEOL 5900 Scanning Electron Microscope (SEM).

Results and Discussion

Self-Extinguishing Time (SET)

The self extinguishing time (SET) of electrolyte with increasing TPP concentration is summarized in Table 1. The baseline electrolyte 1 (BL1, 1.2 M $LiPF_6$ in EC/EMC

3:7 vol.%) shows high flammability with an SET of 23 seconds. Electrolyte with 5% TPP does not show appreciable decrease in flammability. However, incorporation of 10% - 15% TPP results in a significant reduction in SET (9 **s**). SET experiments were also conducted on solvent blends without $LiPF_6$ and the trends in flammability reduction were very similar.

Flash Point (FP)

The flash points (FP) of solvent blends incorporating TPP are provided in Table 2. The FP values of all solvents blends are very similar. The FP values correlate with the expected FP of EMC and suggest that TPP does not significantly alter the composition of the vapor phase above the cup. The significant differences in the quantity of reduced flammability when comparing SET and FP data with added TPP suggest that the development of additional straightforward flammability measurements would be beneficial. This also supports that the primary flame retarding action of the triphenyl phosphate is dependent upon its decomposition, either due to the formation of radical scavenging species or the formation of a thermal barrier of char, which would not be as significant in the flash point test.

Ionic Conductivity

The ionic conductivity of 1.2 M $LiPF_6$ in 3:7 EC/EMC (vol.%) compared to 1.0 M $LiPF_6$ in 3:6:1 EC/EMC/TPP (wt. %) between -60°C and 30°C is depicted in Figure1. Addition of 10% TPP results in a slight decrease in the conductivity of the

electrolyte. The decrease is attributed to a reduction in Li ion transport as a result of TPP incorporation. The difference in conductivity between BL1 and electrolyte with 10 % TPP becomes smaller with decreased temperature.

Cyclic Voltammetry

The cyclic voltammogram (CV) of the BL1 electrolyte and the electrolyte with 10 % TPP and 15 % TPP are shown in Figure 2. During the first potential sweep of the BL1 electrolyte, no reduction peaks are observed above 0.5 V vs. Li. The first potential sweep of electrolytes containing 10 % TPP and 15 % TPP contains a reduction peak at 1.8 V which is not present during the subsequent second and third potential sweeps. In addition, the current intensity of the peak increases with increasing concentration of TPP. This indicates that TPP is reduced on the anode surface but does not adversely affect the formation of a stable anode SEI.

Electrochemical Performance of Cells with Triphenyl Phosphate

Lithium ion coin cells containing an MCMB anode and $LiNi_{0.8}Co_{0.2}O_2$ cathode were prepared with BL1 electrolyte and electrolyte with 5, 10, and 15 % TPP (Figure 3) to evaluate the effect of TPP on the electrochemical performance. Cells containing electrolyte with 5 and 10% TPP have comparable discharge capacity (~155 mAh/g) to cells with BL1 electrolyte (~165 mAh/g). Continued cycling (35 cycles) results in a small increase in the discharge capacity fade for cells containing 5 and 10 % TPP. The initial capacity is lower and the capacity fade upon cycling is more pronounced in

cells with 15 % TPP (~145 mAh/g) as compared to the BL1 electrolyte. It should be noted that although more pronounced capacity decline is observed in these experimental cells, good cycle life performance has been observed in larger prototype cells (7Ah), being comparable with cells containing electrolytes with lower concentrations of TPP.[23]

Performance Characterization of Three-Electrode Experimental Cells with Electrolytes Containing Triphenyl Phosphate

Three electrode cells consisting of MCMB anodes and $LiNi_{0.8}Co_{0.2}O_2$ cathodes were fabricated containing a baseline electrolyte (BL2, 1.0M $LiPF_6$ in EC+EMC (20:80 vol %) and electrolytes with increasing concentration of triphenyl phosphate (i.e., 5, 10, and 15% by volume). In the preparation of these electrolytes the ethylene carbonate content was held constant (at 20% by volume) and the ethyl methyl carbonate content was adjusted accordingly. As illustrated in Table 3, very comparable reversible capacities and irreversible capacities were obtained for all cells, indicating that the incorporation of TPP into the electrolyte does not adversely impact the initial specific capacity. It should be noted that the small observed differences in reversible capacity are not entirely attributable to electrolyte effects, but rather owing to cell to cell variability (i.e., < 5% variation in electrode weights). As shown in Figure 4, when the potentials of the MCMB anodes are observed during the first charge of the formation process, there is no significant reactivity with increasing TPP content and they behave in a similar fashion to the baseline solution soon adopting voltages indicative of lithium intercalation rather than excessive reductive

decomposition of the additive. This suggests that if TPP is participating in the film formation process it is resulting in the formation of a protective film, rather than reacting continually.

After completing the formation cycling and electrochemical characterization of the cells (discussed in the sections below), the cells were subjected to low temperature discharge rate characterization. This testing consisted of charging the cells at room temperature and discharging the cells at -20°C at various rates. As illustrated in Table 4, a noticeable decrease in the discharge rate capability was observed at low temperature with increasing TPP content. This is partly attributed to a decrease in the conductivity of the electrolyte solutions with increasing TPP content. As discussed below, the decreased rate capability is also attributed to decreased lithium intercalation/de-intercalation kinetics at the interfaces, since increased film and charge transfer resistances are observed during the measurement of electrochemical kinetics parameters.

Tafel Polarization Measurements of Three-Electrode Experimental Cells with Electrolytes Containing Triphenyl Phosphate

To determine the lithiation/de-lithiation kinetics of both the anode and the cathodes in the three-electrode cells, Tafel polarization measurements were performed on the MCMB/ $LiNi_{0.8}Co_{0.2}O_2$ cells at 20^o, 0^o, and -20^oC. These measurements were performed after the cells completed the formation cycling and were fully charged (i.e., the open circuit potential was above 4.08 V). To approximate steady-state conditions,

the measurements were performed under potentiodynamic conditions with slow scan rates (0.2 mV/sec). During the polarization of 150 mV vs. the open-circuit potentials, there is noticeable mass-transfer interference on the charge-transfer process. Corrections were therefore applied for this mass transfer interface, by electrode potential against Log $[I/\{(1-(I/I_l)\}]$, where I_l is the limiting current estimated from extrapolation. The rate parameters for the intercalation/de-intercalation of lithium (i.e., the exchange current and transfer coefficients), were calculated from the intercept and the slope of the mass-transfer corrected plots.[24]

From the exchange current densities listed in Table 5, it is clear that the anode kinetics are nearly comparable for the baseline electrolyte (0.51 mA/cm^2) and the electrolyte with 10% TPP content (0.57 mA/cm^2). However, decreased kinetics were observed at the MCMB anode when utilizing an electrolyte with 15% TPP (0.46 mA/cm^2). These results suggest that increasing TPP content results in interfacial surface films that impede the lithium kinetics and is also accompanied by decreased ionic conductivity of the electrolyte, which will be reflected by decreased limiting currents. In contrast to the anode kinetics which are not significantly altered even though TPP contributed to the SEI, the cathode kinetics are noticeably reduced upon incorporation of TPP into the electrolyte, for example from 1.15 mA/cm^2 for the baseline up to 0.59 mA/cm^2 for 10% TPP and 0.22 mA/cm^2 for 15% TPP. Similar trends are observed upon evaluating the cells at lower temperature, with the electrolyte with 10% TPP content also displaying decreased lithium intercalation and de-intercalation kinetics compared with the baseline. As shown in Figure 5, when Tafel measurements were performed at -20^{o} C on the MCMB anodes, the following trend in

the anode kinetics was observed (in decreasing amount): $LiPF_6$ in EC+EMC (20:80) > $LiPF_6$ in EC+EMC+TPP (20:70:10) > $LiPF_6$ in EC+EMC (20:65:15). A similar trend in the electrode kinetics was observed when Tafel measurements were performed on the $LiNi_{0.8}Co_{0.2}O_2$ cathodes, as shown in Figure 6. In addition to resulting in reduced ionic conductivity, these results support the contention that the TPP is being incorporated into the cathode surface films as well, which is supported by the ex-situ analysis of the electrode harvested from the coin cells discussed in the section below.

Electrochemical Impedance Spectroscopy (EIS) Measurements of Three-Electrode Experimental Cells with Electrolytes Containing Triphenyl Phosphate

In an attempt to further understand the effect that triphenyl phosphate has upon the electrode/electrolyte interface, EIS measurements were performed on each individual electrode, as well as the full cell, by utilizing the reference electrode. In the interpretation of the data, an equivalent circuit consisting of a series resistance, R_s, a parallel resistor-capacitor network (for film capacitance C_f and film resistance R_f) in series for the high frequency relaxation loop, a resistor-capacitor parallel network in series for the low frequency relaxation loop, which is represented by a double-layer capacitance C_{dl} in parallel with as series combination of charge transfer resistance R_{ct}, and a Warburg impedance (w) representing the slow solid state diffusion of lithium ions in the bulk.[25-28] It is generally held that the high frequency relaxation loop is associated with the surface film between the electrolyte and the electrode, whereas the low frequency relaxation loop is correlated to the charge transfer resistance. These

data were analyzed using the equivalent circuit described above and Z Simpwin software.

When EIS measurements were performed on the MCMB anodes after formation, as shown in Figure 7, a noticeable increase in the series resistance is observed with increasing TPP content, especially when 15% is added. This increase is primarily attributable to the decrease in ionic conductivity of the electrolyte solution, due to the addition of TPP, which increases the viscosity and lowers the ionic mobility. The trends in the film resistance and the charge transfer resistances are not as clear as expected. Part of this may be attributed to the interference of the mass transfer on the charge transfer kinetics (as was also seen in the Tafel plots), and the non-ideal Warburg impedance overlapping with the charge transfer relaxation loop. In general, there is an increase in the film and charge transfer resistances with addition of TPP, being again most dramatic for the electrolyte with 15% content (Table 6). This suggests that TPP is altering the SEI film hindering facile lithium kinetics due to a more resistive nature compared to the baseline solution. The addition of TPP may also influence the solvation and coordination of Li ions in solution, in turn influencing the de-solvation characteristics. However, the extent of this potential interaction and how the subsequent de-solvation characteristics may influence the charge transfer characteristics[29] requires further study. When EIS measurements were performed on the $LiNi_{0.8}Co_{0.2}O_2$ cathodes, only modest increases in the film and charge transfer resistance were observed with the cell containing the electrolyte with 10% TPP. However, the cell with the electrolyte possessing 15% TPP resulted in much higher series, film, and especially charge transfer resistance, as illustrated in Figure 8.

Scanning Electron Microscopy (*SEM)*

Scanning electron microscope (SEM) images of MCMB anodes and $LiNi_{0.8}Co_{0.2}O_2$ cathodes from cycled full cells with LB1 electrolyte and electrolyte with 10 % TPP are provided in Figures 9-10. Anodes extracted from full cells cycled with BL1 electrolyte and electrolyte containing 10 % TPP have very similar surface morphology. Cathodes extracted from full cells with BL1 and 10 % TPP electrolytes also have very similar surface structure. The results suggest that the incorporation of TPP does not significantly affect the bulk structure of the materials.

X-ray Photoelectron Spectroscopy (*XPS)*

XPS analysis of the surface of electrodes extracted from cells containing BL1 and TPP-containing electrolytes was conducted to understand the role of TPP on the structure of surface films on the electrode materials. Elemental surface concentrations of the anodes are provided in Table 7. After 35 cycles, the concentration of C decreases while the concentration of O and F increase relative to the fresh anode, consistent with the formation of an SEI on the anode. Incorporation of 5 % TPP results in an increase in the concentration of O and a decrease in the concentration of F, but further increases in the concentration of TPP result in a decrease in the concentration of O and increase in the concentration of C suggesting that the composition of the anode SEI is being altered by the addition of TPP. The P elemental concentrations remain small for all samples suggesting that TPP is not being incorporated into the anode SEI.

The XPS spectra of anodes extracted from full cells cycled with TPP electrolyte are depicted in Figure 11. The fresh anode contains peaks for graphite at 284.3 eV and two peaks for PVDF at 286.4 and 290.5 eV in the C1s spectrum. The corresponding F1s peak for PVDF is observed at 688 eV and a small peak is observed in the O1s spectrum at 533 eV characteristic of residual oxygenated impurities on the graphite surface. The C1s spectrum of cycled anodes contains a new peak at 289.5 eV, consistent with the presence of C=O containing species such as lithium alkyl carbonates, in addition to the peaks characteristic of graphite and PVDF, suggesting that the anode SEI is relatively thin. The C1s spectrum does not change significantly upon incorporation of TPP indicating that TPP does not significantly alter the carbon containing components. The F1s spectrum contains peaks for PVDF (688 eV) and LiF (684.5 eV). LiF is a common component of anode SEIs resulting from the decomposition of $LiPF_6$. The relative concentration of LiF, compared to PVDF, decreases with increasing TPP concentration suggesting that the TPP may inhibit the decomposition of $LiPF_6$.[1, 30] The O1s spectrum shows a mix of C=O and C-O bonds at 531.5 eV confirming the production of a mix of lithium carbonate (Li_2CO_3) and lithium alkyl carbonates. The P2p spectrum contains evidence of lithium fluorophosphates ($Li_xPO_yF_z$) at 133.5 eV while the corresponding F1s peaks for $Li_xPO_yF_z$ coincides with the peak for PVDF at 688 eV.

Elemental surface concentrations of cathodes with TPP based electrolyte are shown in Table 8. After 35 cycles, the concentration of C decreases while the concentration of O and F increase for cells cycled with the BL1 electrolyte. The incorporation of TPP alters the elemental concentration on the surface of the cathode.

The concentration of C and O are increased while the concentration of F is decreased with increasing TPP concentration. In addition, P and Ni concentrations remain low for all electrodes.

XPS spectra of cathodes extracted from full cells cycled with TPP electrolyte are presented in Figure 12. The C1s spectrum of the fresh cathode contains peaks characteristic of graphite (284.3 eV) from the conductive carbon dilutant and PVDF binder (286.4 and 290.5 eV). The F1s spectrum contains a single peak characteristic of PVDF at 688 eV while the O1s spectrum has peaks for lithium carbonate (531.5 eV) and metal oxide (529 eV). Analysis of the cathode extracted from a cell cycled with baseline 1 electrolyte reveal small changes to the cathode surface. The C1s spectrum is similar but the F1s spectrum contains a new peak at 684.5 eV consistent with the presence of LiF and the O1s peak for the metal oxide is decreased consistent with the formation of a cathode surface film. The addition of TPP to the electrolyte further alters the C1s spectra of the extracted electrodes. With increasing concentrations of TPP a gradual decrease in the intensity of the C-F peak at 290.5 eV and C-H peak at 286.4 eV are observed indicating the formation of a cathode surface film covering the PVDF binder. Increasing the concentration of TPP also decreased the intensity of the peak for LiF suggesting less LiF on the cathode surface with added TPP. The decrease in LiF concentration on the cathode is similar to the decreased LiF concentrations on the anode discussed above further supporting the stabilization of $LiPF_6$ in the presence of the Lewis basic TPP.[1,30] The O1s spectra of samples cycled with TPP contain peaks characteristic of Li_2CO_3 and lithium alkyl carbonates at 531.5 eV as well as Li metal oxide at 529 eV.

Conclusions

The effect of the addition of triphenyl phosphate (TPP) as a flame retarding additive for lithium ion battery electrolytes was investigated. The incorporation of TPP into standard carbonate based electrolytes resulted in a significant reduction in the flammability of the electrolyte as determined by self-extinguishing tests (SET). However, the incorporation of TPP did not significantly alter the flash point of the solvent blends, suggesting that the decomposition of TPP (either leading to the char formation or radical scavenging species) is essential to the flame retarding action. TPP incorporation resulted in a slight decrease in the electrolyte conductivity which corresponds to slight increase in the cell impedance especially at low temperature (-20 ^{o}C). However, addition of up to 10 % TPP did not significantly reduce the cycling performance and capacity retention of lithium ion cells. When EIS measurements were performed, a noticeable increase in the series, film, and charge transfer resistances was observed, especially on the MCMB anodes, suggesting that TPP is altering the structure of the SEI film hindering facile lithium kinetics due to a more resistive nature. Decreased kinetics were also observed at both electrodes with an electrolyte with 15% TPP especially at lower temperatures, as determined by Tafel polarization measurements, being attributed to lower ionic conductivity as well as the presence of TPP altering the surface layers of both electrodes. Post-mortem XPS and SEM analysis of the electrode surfaces suggest that the addition of up to 10 % TPP results in small changes to the composition of the surface films but does not significantly interfere with the anode SEI film formation process. In summary, TPP is a promising flame retarding additive for lithium ion batteries with minimal deleterious

effect on the electrode kinetics performance, but may result in improved safety for the large format cells.

Acknowledgement

This research project was funded by the NASA Rhode Island Space Grant Consortium and NASA EPSCoR. Some of the work described here was carried out at the Jet Propulsion Laboratory, California Institute of Technology, under contract with the National Aeronautics and Space Administration (NASA) and under sponsorship of the NASA-Space Exploration Systems (SPS) program. Technical support was provided by Yardney Technical Products, Inc.

References

1. S. Dalavi, M. Xu, B. Ravdel, L. Zhou, and B. L. Lucht, *J. Electrochem. Soc*., **157**, A1113 (2010).

2. K. Xu, *Chem. Rev.*, **104**, 4303 (2004).

3. E.G. Shim, T.H. Nam, J.G. Kim, H.S. Kim, and S.I. Moon, *J. Power Sources,* **172**, 919 (2007).

4. H. F. Xiang, H. Y. Xu, Z. Z. Wang, and C. H. Chen, *J. Power Sources,* **173**, 562 (2007).

5. E.G. Shim, T.H. Nam, J.G. Kim, H.S. Kim, and S.I. Moon, *Electrochimica Acta.,* **54,** 2276 (2009).

6. X. Wang, E. Yasukawa, S. Kasuya, *J. Electrochem. Soc.,* **148,** A1058 (2001)

7. Y. E. Hyung, D. R. Vissers, and K. Amine, *J. Power Sources*, **383,** 119 (2003).

8. K. A. Smith, M. C. Smart, G. K. S. Prakash, and B. V. Ratnakumar, *ECS Trans.*, **16** (35), 33 (2009).

9. M. C. Smart, F. C. Krause, C. Hwang, W. C. West, J. Soler, G. K. S. Prakash, and B. V. Ratnakumar, *ECS Trans*., **35** (13), 1 (2011).

10. X. Xia, P. Ping, and J. R. Dahn *J. Electrochem. Soc.,* **159**, A1460 (2012).

11. P. Ping, Q. S. Wang, J. H. Sun, X. Xia, and J. R. Dahn *J. Electrochem. Soc.,* **159**, A1467 (2012).

12. K. Xu, M. S. Ding, S. Zhang, J. L. Allen, T. R. Jow, *J. Electrochem. Soc.*, **149**, A622, (2002).

13. K. Xu, S. Zhang, J. L. Allen, T. R. Jow, *J. Electrochem. Soc.*, **149**, A1079, (2002).

14. K. Xu, M. S. Ding, S. Zhang, J. L. Allen, and T. R. Jow, *J. Electrochem. Soc.*, **150**, A161 (2003).

15. J. K. Feng, X. P. Ai, Y. L. Cao, and H. X. Yang, *J. Power Sources*, **177**, 194 (2008).

16. A. Granzow, *Acc. Chem. Res.*, **11**, 177 (1978).

17. X. Wang, E. Yasukawa, and S. Kasuya, *J. Electrochem.Soc.*, **148**, A1058 (2001).

18. D. H. Doughty, E. P. Roth, C. C. Crafts, G. Nagasubramanian, G. Henriksen, and K. Amine, *J. Power Sources*, **146**, 116 (2005).

19. H.F. Xiang, Q.Y. Jin, C.H. Chen, X.W. Ge, S. Guo, J.H. Sun, *J Power Sources*, **174**, 335 (2007).

20. S.-H. Kang, D.P. Abraham, A. Xiao, and B.L. Lucht *J. Power Sources* **175** 526 (2008).

21. A. M. Andersson, D. P. Abraham, R. Hasch, S. MacLaren, J. Liu, and K. Amine, *J. Electrochem. Soc.*, **149**, A1358 (2002)

22. W. Li and B. L. Lucht *J. Electrochem. Soc.*, **153**, A1617 (2006).

23. M. C. Smart, L. D. Whitcanack, F. C. Krause, C. Hwang, R. V.Bugga, S. Santee, F. J. Puglia, and R. Gitzendanner, 45th Power Sources Conference, Las Vegas, NV, June 11-14, 2012 (p. 517-520).

24. M. C. Smart, B. L. Lucht, S. Dalavi, F. C. Krause, and B. V. Ratnakumar, *J. Electrochem. Soc.*, **159**, A739 (2012).

25. A Funabiki, M. Inaba, Z Ogumi, S. Yuasa, J. Otsuji, and A. Tasaka, *J. Electrochem. Soc.*, **145**, 174 (1998).

26. M. Wagner, *Electrochim. Acta*, **42**, 1623 (1997).

27. B. A. Boukamp, *Solid State Ionics*, **20**, *31* (1986).

28. M. C. Smart, B. V. Ratnakumar, J. F. Whitacre, L. D. Whitcanack, K. B. Chin, M. D. Rodriguez, D. Zhao, S. G. Greenbaum, and S. Surampudi, *J. Electrochem. Soc.*, **152**, A1096 (2005).

29. K. Xu, A. Von Cresce, and U. Lee, *Langmuir*, **26**, 11538 (2010).

30. W. Li, C. Campion, B. L. Lucht, B. Ravdel, J. DiCarlo, and K. M. Abraham *J. Electrochem Soc.,* **152**, A1361 (2005).

Electrolyte Solutions	S.E.T (s)	σ (s)
Std. - {1.2M $LiPF_6$ (EC/EMC) (3:7) vol.%}	**23**	**2.6**
5% TPP - {1.0M $LiPF_6$ (EC/EMC/TPP) (3:6.5:0.5) wt. %}	**23**	**2.3**
10% TPP - {1.0M $LiPF_6$ (EC/EMC/TPP) (3:6:1) wt.%}	**9**	**2.2**
15% TPP - {1.0M $LiPF_6$ (EC/EMC/TPP) (3:5.5:1.5) wt.%}	**9**	**1.2**

Table 2-1. Self-extinguishing times for electrolytes with TPP

Solvent Mixture	Flash Point (°C)
Std. – {EC/EMC 3:7 wt.%}	**29.7**
5% TPP– {EC/EMC + 5 wt.%TPP}	**29.7**
10% TPP –{EC/EMC + 10 wt.% TPP}	**30.7**
15% TPP – {EC/EMC + 15 wt.% TPP}	**31.0**

Table 2-2. Flash Points of solvent blends.

Electrolyte Type	Charge Capacity (Ah) 1st Cycle	Discharge Capacity (Ah) 1st Cycle	Irrev. Capacity (Ah) 1st Cycle	Coulombic Efficiency 1st Cycle	Charge Capacity (Ah) 5th Cycle	Discharge Capacity (Ah) 5th Cycle	Cumulative Irrev. Capacity (1st -5th Cycle)	Coulombic Efficiency 5th Cycle
1.0M $LiPF_6$ in EC+EMC (20:80 v/v %)	0.4682	0.4044	0.064	86.39	0.4013	0.3914	0.1136	97.53
1.0M $LiPF_6$ in EC+EMC+TPP (20:65:5 v/v %)	0.4561	0.3977	0.058	87.19	0.3898	0.3894	0.0734	99.88
1.0M $LiPF_6$ in EC+EMC+TPP (20:70:10 v/v %)	0.4705	0.3978	0.073	84.55	0.3969	0.3819	0.1449	96.20
1.0M $LiPF_6$ in EC+EMC+TPP (20:75:15 v/v %)	0.4645	0.4037	0.061	86.91	0.4027	0.3980	0.0881	98.84

Table 2-3. Charge-discharge (formation) characteristics of experimental MCMB/ $Li_xNi_yCo_{1-y}O_2$ lithium-ion cells containing electrolytes with and without triphenyl phosphate.

		1.0 M $LiPF_6$ in EC+EMC (20:80 v/v %)		1.0 M $LiPF_6$ in EC+EMC+TPP (20:70:10 v/v %)		1.0 M $LiPF_6$ in EC+EMC+TPP (20:65:15 v/v %)	
Temp.	Current (mA)	Capacity (Ah)	Percent (%)	Capacity (Ah)	Percent (%)	Capacity (Ah)	Percent (%)
23°C	25	0.3914	100.00	0.3819	100.00	0.3980	100.00
- 20°C	25	0.3370	86.12	0.3208	84.00	0.2436	61.19
	50	0.3206	81.92	0.2579	67.54	0.1889	47.45
	100	0.3044	77.79	0.1354	35.45	0.0944	23.72
	150	0.2913	74.44	0.0429	11.23	0.0419	10.53

Table 2-4. Summary of the discharge characteristics experimental MCMB/ $Li_xNi_yCo_{1-y}O_2$ lithium-ion cells containing various electrolytes at -20°C. Cells were charged at 20°C.

FRA Content	Anode i_o, mA/cm^2			Cathode i_o, mA/cm^2		
	25^{o}C	0^{o}C	-20^{o}C	25^{o}C	0^{o}C	-20^{o}C
0 %	0.51	0.26	0.08	1.15	0.31	0.06
10 %	0.57	0.28	0.06	0.59	0.27	0.06
15 %	0.46	0.23	0.04	0.22	0.14	0.02

Table 2-5. Summary of the electrode kinetic data obtained from Tafel polarization measurements.

		25°C			0°C			-20°C		
	FRA (%)	R_f (Ω)	R_{ct} (Ω)	I_o, mA/cm^2	R_f (Ω)	R_{ct} (Ω)	I_o, mA/cm^2	R_f (Ω)	R_{ct} (Ω)	I_o, mA/cm^2
MCMB	0	0.03	0.02	10.93	0.21	0.28	0.59	1.08	0.44	0.37
	10	0.12	0.17	0.99	0.31	0.20	0.82	-	-	-
	15	0.10	-	16.69	0.31	-	0.42	1.21	0.36	0.46
$LiNiCoO_2$	0	0.08	0.05	3.28	0.15	0.25	0.73	1.10	0.14	1.31
	10	-	0.03	5.12	0.26	1.03	0.18	-	-	-
	15	0.10	0.15	1.09	0.09	0.90	0.20	10.27	-	-

Table 2-6. Summary of the electrochemical parameters obtained from EIS measurements.

	C 1s (%)	O 1s (%)	F1s (%)	P 2p (%)
Fresh Anode	70	4	26	N/A
Std. - 1.2M LiPF6 EC/EMC (3:7) vol.%	40	24	34	2
5% TPP - 1.0M $LiPF_6$ EC/EMC/TPP (3:6.5:.5) wt.%	41	33	25	1
10% TPP - 1.0M $LiPF_6$ EC/EMC/TPP (3:6:1) wt.%	52	22	25	1
15% TPP - 1.0M LiPF6 EC/EMC/TPP (3:5.5:1.5) wt.%	52	18	30	1

Table 2-7. Elemental concentration of C, O, F, P, on the anode surface using TPP FR electrolyte.

	C 1s (%)	O 1s (%)	F 1s (%)	P 2p (%)	Ni 1s (%)
Fresh Cathode	58	10	32		
Std. -1.2M LiPF6 EC/EMC (3:7) vol.%	47	12	36	1	4
5% TPP -1.0M $LiPF_6$ EC/EMC/TPP (3:6.5:.5)wt.%	52	18	26	1	3
10% TPP -1.0M $LiPF_6$ EC/EMC/TPP (3:6:1) wt.%	61	17	19	1	2
15% TPP -1.0M LiPF6 EC/EMC/TPP (3:5.5:1.5) wt.%	66	16	12	1	4

Table 2-8. Elemental concentration of C, O, F, P, and Ni on the cathode surface using TPP FR electrolyte.

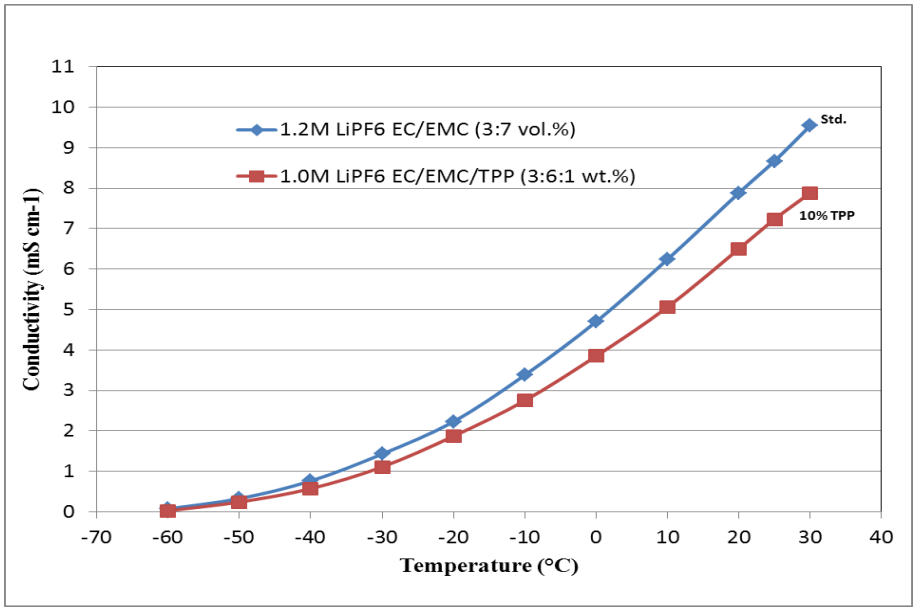

Figure 2-1. Ionic conductivity of electrolyte (1.2 M $LiPF_6$ in EC/EMC (3:7 vol)) with and without triphenyl phosphate (1.2 M $LiPF_6$ in EC/EMC/TPP (3:6:1 vol)) between +30 and - 60 ^{o}C

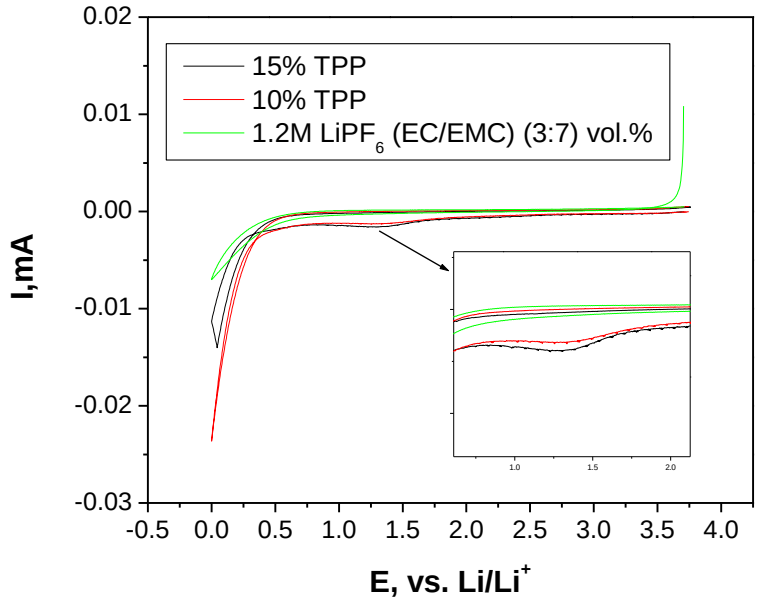

Figure 2-2. Combined 1st Potential Sweep-Cyclic Voltammogram of 1.2 M $LiPF_6$ in EC/EMC (3:7 vol, BL1) vs. EC/EMC/TPP (3:6:1 vol) vs. EC/EMC/TPP (3:5.5:1.5).

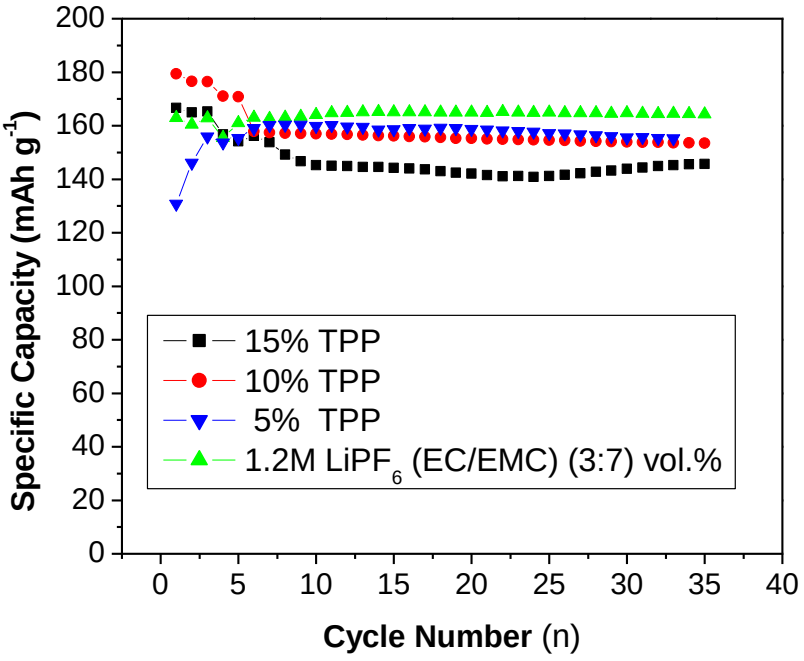

Figure 2-3. Cycling Performance of MCMB/$LiNiCoO_2$ full cells utilizing 1.2 M $LiPF_6$ in EC/EMC (3:7 vol), EC/EMC/TPP (3:6.5:0.5 vol), EC/EMC/TPP (3:6:1 vol), and EC/EMC/TPP (3:5.5:1.5).

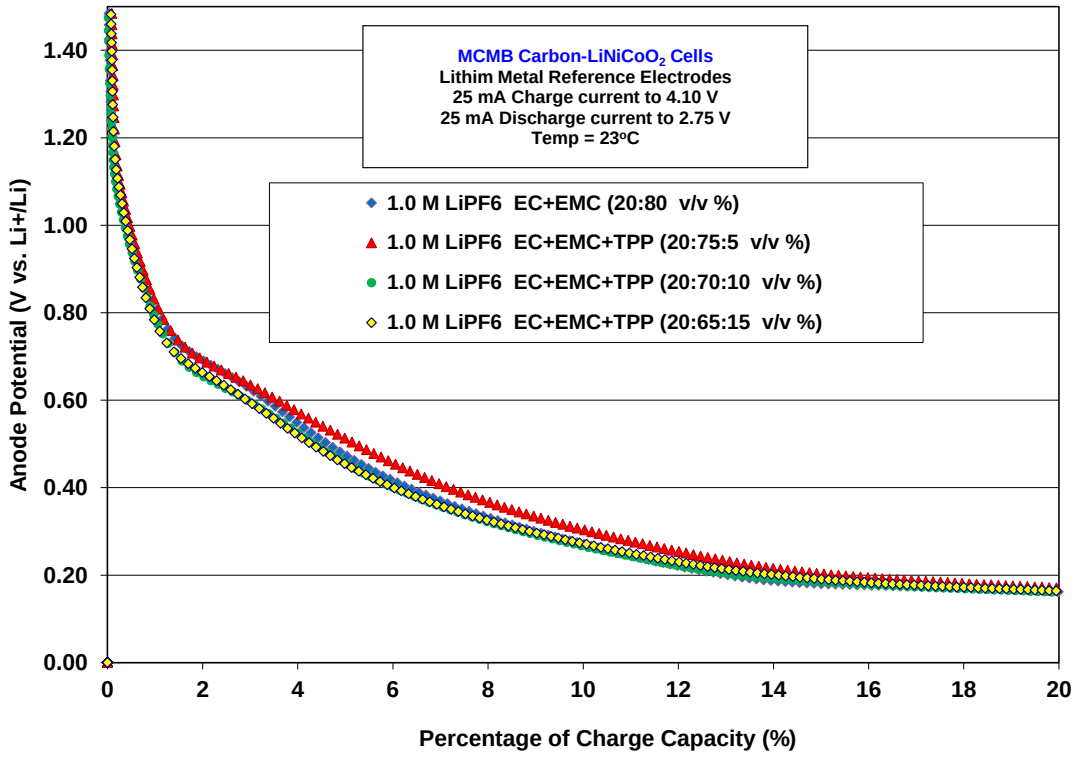

Figure 2-4. The anode potential (V vs. Li_+/Li) of MCMB/ $LiNi_{0.8}Co_{0.2}O_2$ lithium-ion cells containing electrolytes containing varying amounts of triphenyl phosphate during the first charge of the formation process, 1.0 M $LiPF_6$ in EC/EMC (2:8 vol), EC/EMC/TPP (2:7.5:0.5 vol), EC/EMC/TPP (2:7:1 vol), and EC/EMC/TPP (2:6.5:1.5).

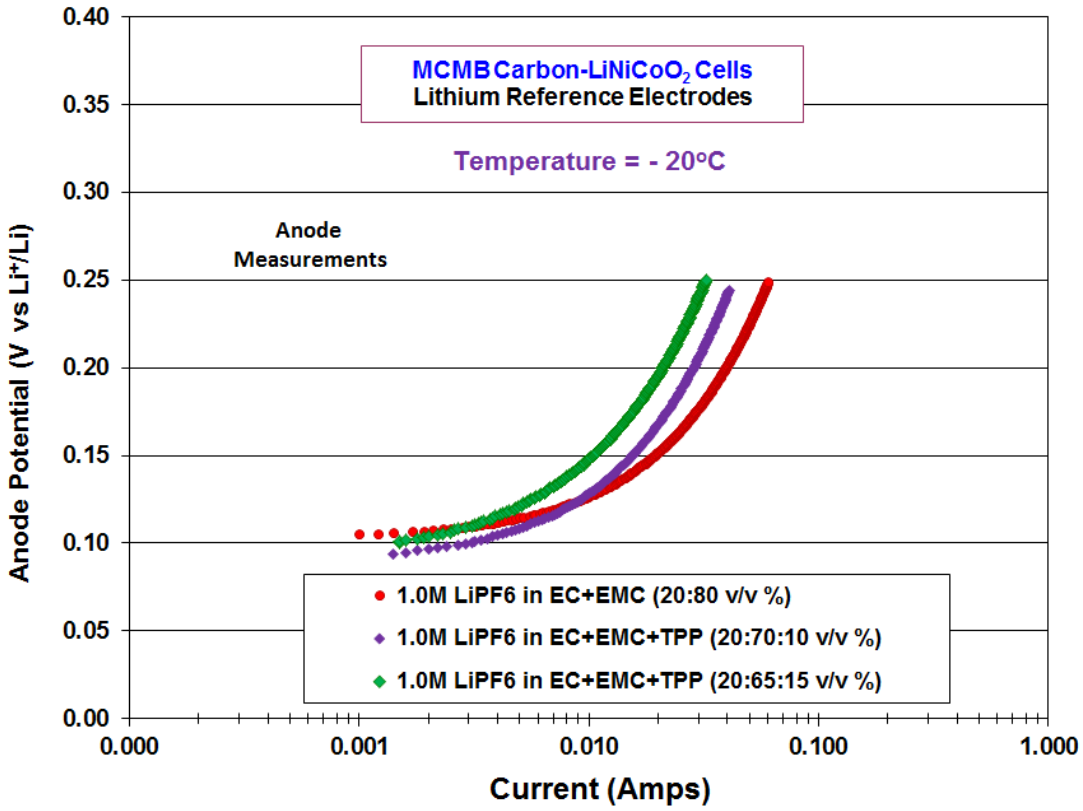

Figure 2-5. Tafel polarization measurements at - 20°C of MCMB electrodes from MCMB/ $LiNi_{0.8}Co_{0.2}O_2$ lithium-ion cells containing electrolytes containing varying amounts of triphenyl phosphate, 1.0 M $LiPF_6$ in EC/EMC (2:8 vol), EC/EMC/TPP (2:7:1 vol), and EC/EMC/TPP (2:6.5:1.5).

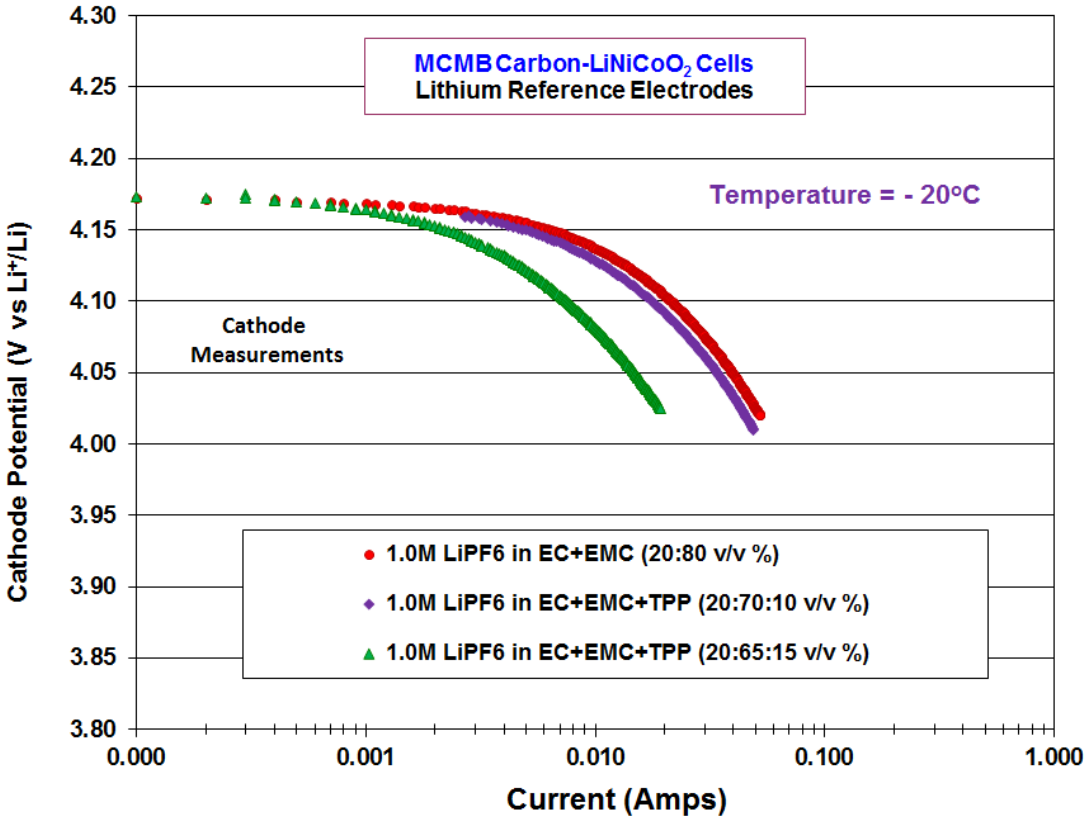

Figure 2-6. Tafel polarization measurements at - 20°C of $LiNi_{0.8}Co_{0.2}O_2$ electrodes from MCMB/ $LiNi_{0.8}Co_{0.2}O_2$ lithium-ion cells containing electrolytes containing varying amounts of triphenyl phosphate, 1.0 M $LiPF_6$ in EC/EMC (2:8 vol), EC/EMC/TPP (2:7:1 vol), and EC/EMC/TPP (2:6.5:1.5).

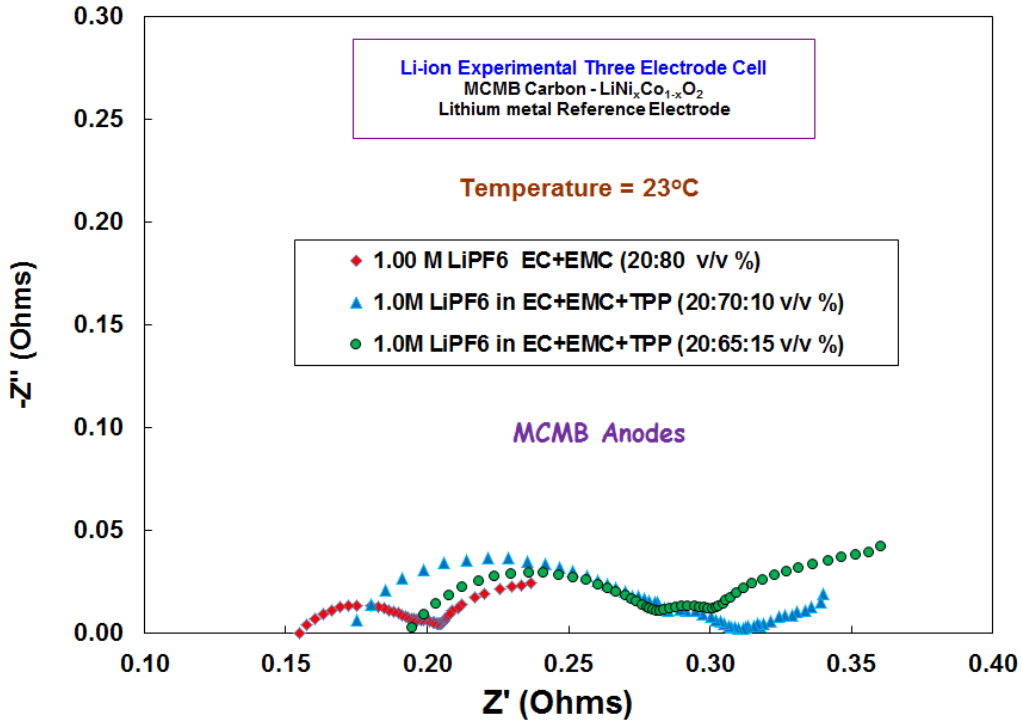

Figure 2-7. Electrochemical impedance spectroscopy (EIS) measurements at 23°C of MCMB electrodes from lithium-ion cells containing electrolytes with and without triphenyl phosphate, 1.0 M $LiPF_6$ in EC/EMC (2:8 vol), EC/EMC/TPP (2:7:1 vol), and EC/EMC/TPP (2:6.5:1.5).

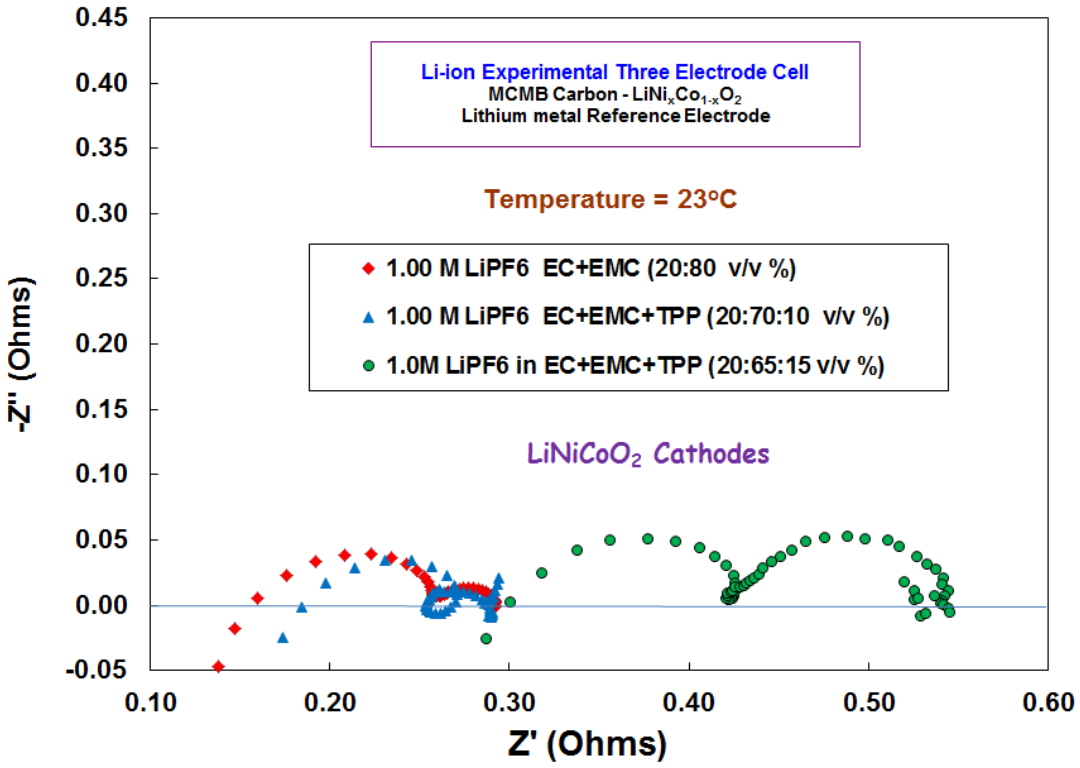

Figure 2-8. Electrochemical Electrochemical impedance spectroscopy (EIS) measurements at 23°C of $LiNi_{0.8}Co_{0.2}O_2$ electrodes from lithium-ion cells containing electrolytes with and without triphenyl phosphate, 1.0 M $LiPF_6$ in EC/EMC (2:8 vol), EC/EMC/TPP (2:7:1 vol), and EC/EMC/TPP (2:6.5:1.5).

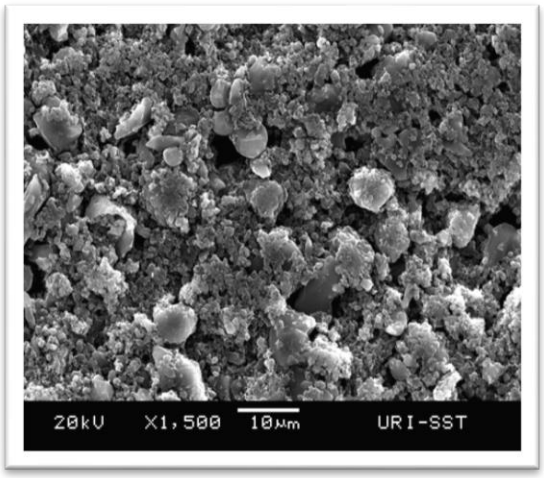

a

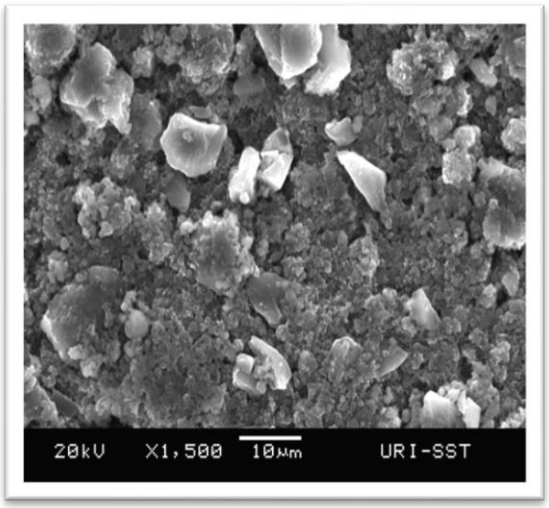

b

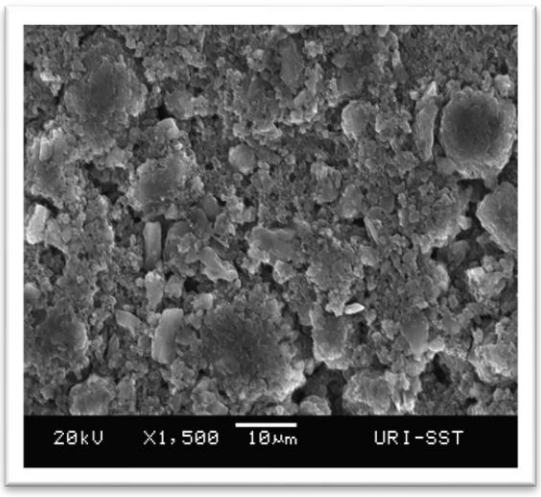

c

Figure 2-9. SEM of MCMB anodes. a) Fresh; b) 1.2 M $LiPF_6$ in EC/EMC (3:7 vol); c) EC/EMC/TPP (3:6:1 vol).

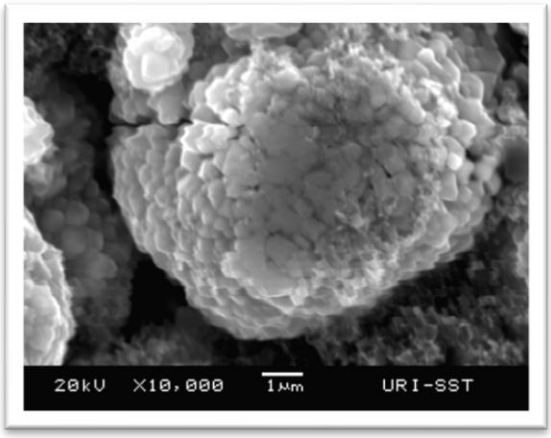

a

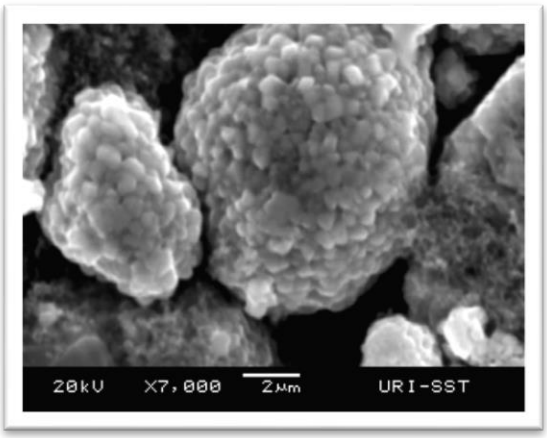

b

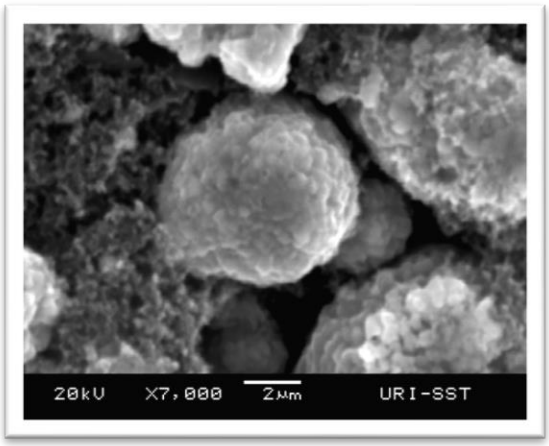

c

Figure 2-10. SEM of $LiNi_{0.8}Co_{0.2}O_2$ cathodes. a) Fresh; b) 1.2 M $LiPF_6$ in EC/EMC (3:7 vol); c) EC/EMC/TPP (3:6:1 vol).

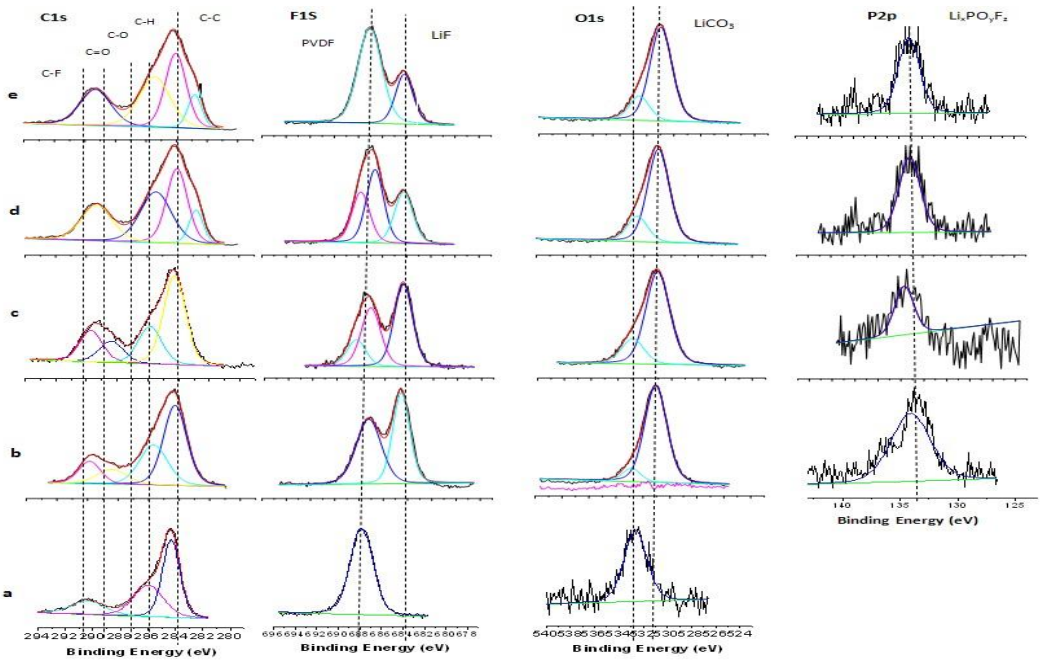

Figure 2-11. XPS Spectra of MCMB anodes. a) Fresh; b) 1.2 M $LiPF_6$ in EC/EMC (3:7 vol); c) EC/EMC/TPP (3:6.5:0.5 vol); d) EC/EMC/TPP (3:6:1 vol); e) EC/EMC/TPP (3:5.5:1.5).

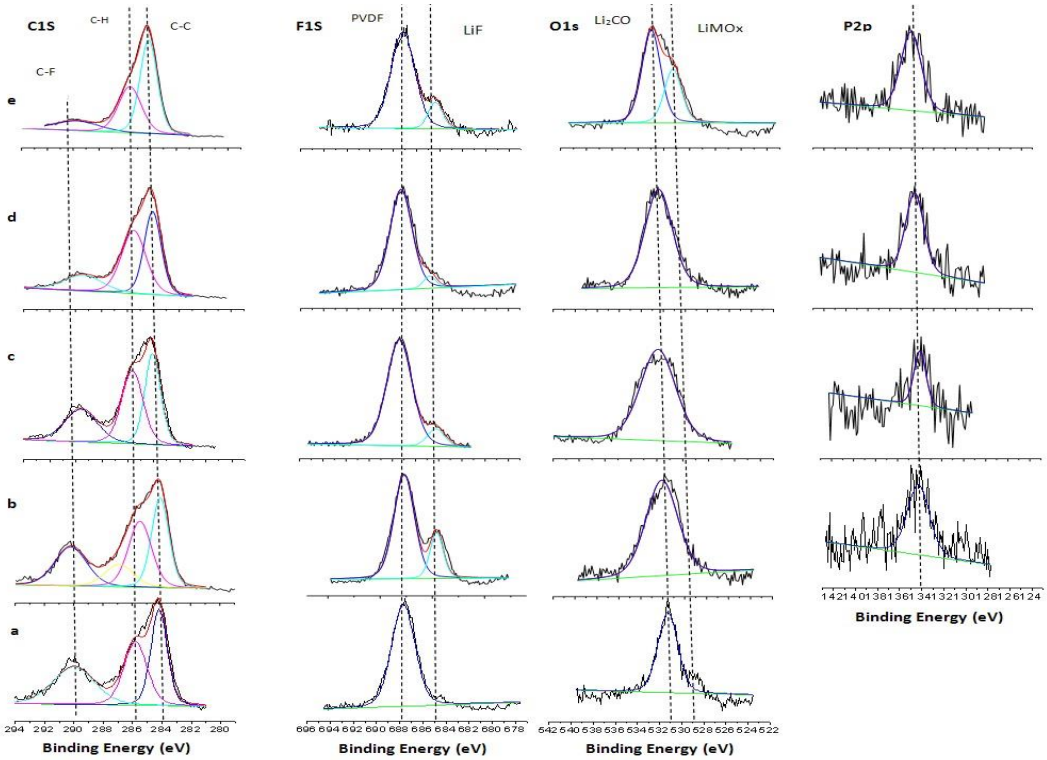

Figure 2-12. XPS Spectra of $LiNi_{0.8}Co_{0.2}O_2$ cathodes a) Fresh; b) 1.2 M $LiPF_6$ in EC/EMC (3:7 vol); c) EC/EMC/TPP (3:6.5:0.5 vol); d) EC/EMC/TPP (3:6:1 vol); e) EC/EMC/TPP (3:5.5:1.5).

Chapter 3

Flame Retardant Cosolvent Incorporation into Lithium-Ion Coin Cells with Thin-film Si Anodes

Ronald P. Dunn,[1] Siva P.V. Nadimpalli,[2] Pradeep Guduru,[2] Brett L. Lucht[1]

[1]*Department of Chemistry, University of Rhode Island,*

Kingston, Rhode Island 02881, USA

[2]*School of Engineering, Brown University,*

Providence, Rhode Island 02912, USA

The following is in preparation for submission to the *Journal of Power Sources*, and is presented here in manuscript format.

Abstract

Due to the inherent flammability and therein risk of thermal runaway associated with standard Li-Ion battery electrolyte, the incorporation of Flame retardant (FR) co-solvents or additives has become a focus for researchers. In addition, there is significant demand for lithium ion batteries with greater energy density. One method to improve the energy density of lithium ion batteries is to increase the capacity of the anode by using silicon. To that end, Triphenyl phosphate (TPP) and Dimethyl methylphosphonate (DMMP) were incorporated into a standard binary $LiPF_6$/ethylene carbonate (EC)/Ethyl methyl carbonate (EMC) electrolyte with and without anode SEI film forming lithium bis(oxalato)borate (LiBOB) to evaluate achievable cycling performances with thin-film silicon/Li half cells. The electrochemical impact of FR incorporation was evaluated via cell cycling and differential chronopotentiometry data analysis. TPP and DMMP incorporated electrolytes show comparable performance to the standard electrolyte. FR incorporation into the standard electrolyte coupled with LiBOB addition results in improved cycling efficiency and capacity retention when cycling in thin-film Si/Li cells. Ex-situ analysis via X-ray photoelectron spectroscopy (XPS) and scanning electron microscopy (SEM) is also performed as to characterize the role of TPP and DMMP in SEI structure and composition.

Introduction

The use of Lithium-ion batteries for portable electronics applications has become widespread in recent years. Li-ion batteries offer higher gravimetric and

volumetric energy density than Ni-Zn, NiCd and NiMH based battery systems. This translates into a longer running and more light-weight rechargeable system.[1,2]

The integration of Li-ion battery systems into platforms with higher energy requirements such as hybrid and electric automobiles has led to the investigation of anode materials with superior energy density. To this end, Silicon has been investigated as a potential anode material due to the higher theoretical specific capacity (3579 mAh/g) compared to the traditional graphite anode (372 mAh/g).[3-5] The demand for Li-ion battery technology for larger scale applications, such as automotive and aerospace, has prompted researchers and developers to address safety issues in Li-ion battery systems. The standard electrolyte in lithium ion batteries is composed of a binary or ternary mixture of ethylene carbonate (EC) with ethyl methyl carbonate (EMC), diethyl carbonate (DEC), or dimethyl carbonate (DMC) and are flammable. The flammability of the electrolyte coupled with the potential for thermal runaway during cell over-charge or over-discharge provides significant safety concerns for large battery systems.[6,7]

Thus there is significant interest in the development of nonflammable electrolytes for lithium ion batteries. One method to develop nonflammable electrolytes is via the incorporation flame retardant (FR) cosolvents/additives. Organophosphates are of high interest due to their natural fire quelling attributes.[8,9] Compounds that have been studied by various groups include 4-Isopropyl Phenyl Diphenyl Phosphate (IPPP)[10], Diphenyloctyl phosphate (DPOF) [11], Triphenyl Phosphate (TPP) [9,12-16], and Dimethyl methylphosphonate (DMMP) [8,17-19]. Triphenyl phosphate (TPP) and Dimethyl methylphosphonate (DMMP) have both shown to be

effective in reducing the flammability of standard electrolytes while offering a comparable electrochemical performance. [8,9,12-19]

Unfortunately, the incorporation of FR co-solvents into standard electrolyte mixtures has frequently resulted in poor capacity retention and poor low temperature performance. This has frequently been attributed to interference of the FR co-solvent with the formation of the anode solid electrolyte interface (SEI). This has prompted many groups to investigate the addition of SEI film stabilizing additives such as vinylene carbonate (VC) and lithium bis(oxalato)borate (LiBOB) in FR electrolytes.[8,9,13-15]

The use of Si anodes as a viable high capacity electrode material poses challenges due to the considerable volume changes (3-4 fold) between the charged and discharged states. [4] The enormous volume changes result in significant internal mechanical stress and subsequent loss of electrical contact between the current collector and Si active material. The overall high level of surface area changes leads to continual reformation of the SEI. This breakdown of the SEI allows for repeated exposure of the electrolyte with the bare electrode. The continuous SEI formation prevalent in the cycling of Si anodes can bring with it large irreversible initial capacity, poor long-term discharge capacity retention/stability and short cell life. In an effort to moderate the effects of the volume changes and resulting breakdown of the Si active material, many groups have focused on decreasing Si particle size within composite materials as well as pursuing thin-film Si anodes. [3-5] The addition of SEI film stabilizing additives such as VC, LiBOB, and fluoroethylene carbonate (FEC) has also been investigated. [5,20,21]

The core focus of many research groups has been the incorporation of FR co-solvents into standard carbonate based lithium ion electrolytes in an effort to reduce flammability without sacrificing electrochemical performance. At the same time, much work has been directed towards the development of silicon anodes to improve the capacity of lithium ion batteries. This study focuses on the electrochemical performance and SEI properties of thin-film Si anodes cycled with flame retardant TPP and DMMP containing electrolytes with and without SEI film stabilizing LiBOB.

Experimental

Battery grade lithium hexafluorophosphate ($LiPF_6$), lithium bis(oxalato)borate (LiBOB), ethylene carbonate (EC), ethyl methyl carbonate (EMC), and dimethyl carbonate (DMC) were obtained from BASF. A standard electrolyte, 1.2 M $LiPF_6$ (EC/EMC) 3:7 (vol.%), was also obtained from BASF and utilized without additional purification. Triphenyl phosphate (TPP) was obtained from Thermo Fisher Scientific at 99% purity. Dimethyl methyl phosphonate (DMMP) was purchased from Sigma-Aldrich dried with sodium hydride and molecular sieves and purified via vacuum distillation. DMMP purity was confirmed via gas chromatography with mass selective detection (GC-MS). FR electrolyte solutions with and without LiBOB were prepared with a constant concentration of $LiPF_6$ and EC. Incorporation of the FR co-solvent coincided with a decrease in the concentration of EMC.

Thin-film Si electrodes were prepared via electron-beam evaporation of Ti onto a Cu foil substrate. A 20 nm thick Si film layer was then deposited via Radio-Frequency (RF)-magnetron sputtering at 150 W in an Ar chamber with approximately

2 mTorr of pressure. The layer of Ti is applied to aide in Si-Cu adhesion.[3,5] Thin-film Si/Li metal coin cells (half cells) were fabricated using electrolyte blends 1-6 in Table 1, in a pure Ar glove box. The Si anode functioned as the working electrode and the Li metal as the counter/reference electrode. A polyolefin separator was utilized and the coin cells were assembled and pressed under a load of 1000 psi.

Cells were cycled at constant-current charge and constant current discharge between 1.3V and 0.05V using an Arbin BT4010 battery cycler at 60 °F (15.5°C). The coin cell cycling protocol followed a formation schedule consisting of one cycle at a C/20 current rate and two subsequent cycles at C/10. The cells were then cycled at a C/5 current rate for 52 cycles. Cycling performance was gathered and coulombic efficiency (cycling efficiency) as well as capacity retention was calculated. Coulombic efficiency is defined as the ratio of discharge capacity or output of the cell to charge capacity or input. Capacity retention is defined as the ratio of discharge capacity at a particular cycle to the initial (1^{st}) cycle discharge capacity.

Ex-situ analysis was conducted following the conclusion of the cycling schedule. Cells were opened in a pure Argon atmosphere glovebox and the cycled Si anodes were extracted and rinsed with DMC to remove residual $LiPF_6$ salt. The rinsed electrodes were then vacuum dried overnight prior to surface analysis. Surface analysis of fresh and cycled Si electrodes was conducted using a JEOL Scanning Electron Microscope (SEM) in an Argon atmosphere chamber. Surface species characterization using X-Ray Photoelectron Spectroscopy (XPS) analysis was performed using a PHI 5500 system and Al Kα radiation. A hydrocarbon (C-H) contamination reference peak of 285 eV was used for spectral adjustment. Multipak

versions 6.1 as well as XPS Peak 4.1 software were utilized for analysis and curve fitting of collected spectra respectively. Gaussian and Lorentzian functions were used for the least squares curve fitting during data processing.

Results and Discussion

Differential Chronopotentiometry

Differential chronopotentiometry analysis of Si/Li cells is consistent with the reduction of LiBOB prior to the reduction of EC, as previously reported (Fig. 1).[21] The DQ/DV results also reveal irreversible reduction of both TPP and DMMP at 1.2 V, very similar voltage to that of LiBOB. Due to similarity of irreversible reduction of LiBOB, DMMP and TPP, a broad irreversible reduction peak is centered at 1.2 V for cells with LiBOB and DMMP or TPP. Thus from the DQ/DV results it is difficult to distinguish if LiBOB alters the reduction of DMMP or TPP. [21, 22]

Electrochemical performance of Si/Li cells

The effect of incorporation of FR co-solvents, TPP and DMMP, into a standard carbonate electrolyte was investigated in Si/Li cells. The capacity retention and coulombic efficiency of the cells during the first 55 cycles is depicted in Fig. 2 while the first cycle efficiencies are provided in Table 2.

Cells cycled with the standard electrolyte have good first cycle efficiency (69 %) and discharge capacity after formation cycles (3100 mAh/g, 5th cycle), but have rapid capacity fade and low coulombic efficiency (93-96 %) during the next 54 cycles. Cells containing the DMMP electrolyte have very similar cycling behavior to the cells

containing standard electrolyte. The first cycle efficiency is 60 % and comparable capacity fade and coulombic efficiency are observed during the next 54 cycles. Cells cycled with the TPP electrolyte have similar first cycle efficiency, 62 %, to cells cycled with standard electrolyte but experience slightly better capacity retention during the next 54 cycles. Cells cycled with the LiBOB containing electrolytes tend to have slightly worse first cycle efficiency but much better capacity retention. Cells cycled with the LiBOB electrolyte have the lowest first cycle efficiency, 46 %, and lowest discharge capacity (~2400 mAh/g) at the end of formation cycling (5th cycle), but these cells retain 87 % of the capacity after 55 cycles. In addition, the coulombic efficiencies of cycles 10 - 55 are greater than 98 %. The incorporation of both LiBOB and FR co-solvent results in further improvement of the cycling performance. The first cycle efficiencies of cells cycled with the TPP and LiBOB electrolyte (62 %) and the DMMP and LiBOB electrolyte (51 %) are improved over the LiBOB electrolyte. In addition, the discharge capacity after formation cycles is higher (3150 mAh/g, 5th cycle), the cycling efficiencies for cycles 10-55 remain high (~98 %), and the capacity retention after 55 cycles is good (83-87 %). The results suggest that the best overall performance of the thin film Si electrodes is observed with flame resistant electrolytes with added LiBOB. In order to develop a better understanding of the source of performance changes as a function of changes in the electrolyte, ex-situ analysis of the surface of the thin film silicon electrodes was conducted.

Scanning electron microscopy (SEM)

SEM imaging of fresh thin-film Si anodes show a smooth surface while Si anodes extracted from Si/Li cells after 55 cycles have observable changes to the

surface consistent with the formation of an SEI (Fig 3a-f). Si anodes cycled with the standard electrolyte, TPP electrolyte, and DMMP electrolyte all show similar increases in surface striations with a relatively thin surface film covering the striations. Si anodes extracted from cells cycled with the LiBOB electrolyte, TPP and LiBOB electrolyte, and DMMP and LiBOB electrolyte, reveal a thick film on the surface of the Si with lesser changes to the surface striations. The thicker surface coverage in the presence of LiBOB is consistent with a thicker SEI on the silicon surface while increased striation in the absence of LiBOB is consistent with more damage to the silicon surface.

X-ray photoelectron spectroscopy (XPS)

XPS analysis of thin-film Si electrodes extracted from cells after 5 and 55 cycles reveal changes in the composition of the anode SEI as a result of the incorporation of FR cosolvents with and without the incorporation of LiBOB as a SEI film forming additive (Fig. 4-5, Tables 3-4). Analysis of the silicon electrode after 5 cycles reveal very low concentrations of Si (< 2 %) for all electrolytes consistent with the generation of a thick SEI passivation layer covering the electrode surface. The decrease in Si concentration is accompanied by a decrease in the O concentration and a large increase in the concentration of F for electrolytes without LiBOB. The electrodes extracted from cells cycled with electrolytes containing added LiBOB have an increase in the concentrations of C and B, while electrolytes containing TPP and DMMP have a slight increase in the concentration of P.[5,8,21,22]

XPS spectra of the fresh thin-film Si anode contains peaks characteristic of pure Si at 99.6 eV and Si-O at 102.3 eV in the Si2p spectrum, Si-O at 532.5 eV in the O1s spectrum, and universal hydrocarbon (C-H) contamination at 285 eV in the C1s spectrum. The XPS spectra of the silicon electrodes after cycling reveal significant changes. Electrodes extracted from cells cycled with standard electrolyte contain peaks in the C1s spectra characteristic of C-O and C=O containing species at, 286.5 and 288.5 eV respectively. The broad peak in the O1s spectrum is also consistent with the presence of C-O (533-534eV) and C=O (532-533eV) containing species. The C1s and O1s peaks are consistent with the presence of lithium alkyl carbonates in the anode SEI as previously reported.[3,5,21] The F1s spectrum contains a very strong peak at 685 eV characteristic of LiF and a shoulder at 687 eV with a corresponding P2p spectrum contains a weak peak at 135 eV characteristic of $Li_xPF_yO_z$. Thus, the SEI generated on the silicon electrode surface in the presence of standard electrolyte is primarily a mixture of lithium alkyl carbonates and LiF with a low concentration of $Li_xPF_yO_z$.[3,5,21] Upon incorporation of the FR co-solvents, DMMP and TPP, only small changes are observed in the element spectra. The C1s, O1s, and F1s spectra are very similar, while a slight increase in intensity and shift to lower energy observed in the P2p spectrum suggesting that the TPP and DMMP are being reduced on the silicon surface. In addition, the Si2p spectrum of the electrode cycled with DMMP electrolyte contains weak peaks characteristic of Si and Si-O. Thus, the incorporation of TPP and DMMP result in small changes to the SEI consistent with the small variation in cycling performance. [5,21,22]

XPS spectra of Si electrodes cycled with the LiBOB electrolyte contain strong C1s peaks at 286.5 and 288.5 eV characteristic of C-O and C=O containing species, but the high intensity of the peak at 288.5 eV is consistent with the presence of a high concentration of lithium oxalate, as previously observed for LiBOB containing electrolytes. [5,8,21,22] The corresponding peak for lithium oxalate is observed in the O1s spectrum at 531-532 eV. The F1s spectrum contains a weak peak at 685 eV consistent with a low concentration of LiF while the B1s spectrum contains a weak peak at 193 eV characteristic of borates.[5,8,22] The XPS spectra of Si electrodes cycled with the DMMP and LiBOB electrolyte and the TPP and LiBOB electrolyte are very similar to the electrodes cycled with the LiBOB electrolyte. The surface contains a high concentration of lithium oxalate and low concentrations of LiF and borates. However, the presence of TPP and DMMP reduction products are observed at 134 eV in the P2p spectrum.

XPS analysis was also conducted on electrodes extracted from cells after 55 cycles and compared to the electrodes after 5 cycles to develop a better understanding of the evolution of the SEI and the role of the SEI in capacity fade (Figure 5, Table 4). The Si electrodes extracted from cells after 55 cycles with standard electrolyte, TPP electrolyte, and DMMP electrolyte have higher concentrations of F and lower concentrations of C and O consistent with additional electrolyte decomposition and an SEI with greater inorganic content.[8.9] The C1s spectra of the electrodes extracted from cells containing the standard electrolyte, the TPP electrolyte and the DMMP electrolyte have significant changes. The intensity of the C1s peak at 286.5 eV is increased consistent with the further deposition of additional C-O containing

decomposition products. However, the changes to the F1s, O1s, Si2p, and P2p element spectra are relatively small. The changes to the SEI are consistent with additional electrolyte decomposition which correlates well with the poor capacity retention observed during cycling.

Alternatively, the Si electrodes extracted from cells containing electrolyte with the LiBOB electrolyte, the TPP and LiBOB electrolyte, and the DMMP and LiBOB electrolyte have only small changes in the element concentrations consistent with a stable SEI. The element spectra of the electrodes extracted after 55 cycles are also very similar to the element spectra after 5 cycles. The small changes to the SEI are consistent with the generation of a stable SEI which correlates with good capacity retention.

Conclusions

The electrochemical performance of thin-film Si anodes cycled with flame retarding electrolytes containing either TPP or DMMP with and without added LiBOB as a SEI stabilizer was investigated. Silicon anodes cycled with standard electrolyte, DMMP electrolyte and TPP electrolyte have poor capacity retention over the first 50 cycles and ex-situ surface analysis reveals significant changes to the composition of the SEI. The changes to the SEI on the Si electrode are consistent with additional electrolyte reduction and poor passivation by the surface film. Silicon electrodes cycled with electrolytes containing the SEI stabilizing additive, LiBOB, have improved capacity retention. The incorporation of both a flame retarding additive, DMMP or TPP, and LiBOB results in the highest discharge capacity and the best

capacity retention. Ex-situ surface analysis suggests that the SEI generated in the presence of added LiBOB has a high concentration of lithium oxalate and a low concentration of LiF. In addition, very small changes occur to the structure of the SEI during the first 55 cycles suggesting that the SEI has good stability. The incorporation of either DMMP or TPP results in the presence of additional phosphorus containing reduction products in the SEI which results in improved cell capacity. Non-flammable electrolytes have been developed for thin film silicon electrodes which allow good cycling performance and the generation of a stable SEI.

Acknowledgement

This research project was funded by the NASA EPSCoR program.

References

1.D. Linden., Handbook of Batteries, fourth ed., McGraw-Hill Professional, New York, 2010.

2. K. Xu, Chem. Rev. 104 (2004) 4303.

3. S.P.V. Nadimpalli., V.A. Sethuraman., S. Dalavi., B.L. Lucht., M.J. Chon., V.B. Shenoy., P.R. Guduru, J. Power Sources. 215, (2012) 145-151.

4. U. Kasavajjula, C. Wang, A.J. Appleby, J. Power Sources 163 (2007) 1003.

5. S. Dalavi, P.R. Guduru, B.L. Lucht, J. Electrochem. Soc. 159 (2012) A642.

6. M. C. Smart, B. V. Ratnakumar, S. Surampudi, J. Electrochem. Soc. 146 (1999) 486-492.

7. K. Xu, M. S. Ding, S. Zhang, J. L. Allen, T. R. Jow, J. Electrochem. Soc. 149 (2002) A622-
A628.

8. S. Dalavi, B.L.Lucht, B. Ravdel, M. Xu, L.Zhou, J. Electrochem. Soc. 157, (2010) A1113-A1120.

9. R.P.Dunn, J. Kafle, F.C.Krause, C.Hwang, B.V.Ratnakumar, M.C.Smart, B.L.Lucht, J. Electrochem. Soc. 159, (2012) A2100-A2108.

10. Q.Wang, J. Sun, X.Yao, C. Chen, Electromchem, Solid State Lett. 8 (9) (2005) A467-A470.

11. E. G. Shim, T. H. Nam, J. G. Kim, H. S. Kim, and S. I. Moon, Electrochimica Acta. 54, (2009) 2276-2283.

12. E. G. Shim, T. H. Nam, J. G. Kim, H. S. Kim, and S. I. Moon, J. Power Sources.172 (2007) 919-924.

13. K. A. Smith, M. C. Smart, G. K. S. Prakash, and B. V. Ratnakumar, ECS Trans. 16(35) (2009) 33-41.

14. M. C. Smart, F. C. Krause, C. Hwang, W. C. West, J. Soler, G. K. S. Prakash, and B. V. Ratnakumar, ECS Trans. **35**(13) (2011) 1-11.

15. E. G. Shim, T. H. Nam, J. G. Kim, H. S. Kim, S. I. Moon, J. Power Sources, 172 (2007) 901-907.

16. Y. E. Hyung, D. R. Vissers, and K. Amine, J. Power Sources, 119-121 (2003) 383-387.

17. H. F. Xiang, Q. Y. Jin, C. H. Chen, X. W. Ge, S. Guo, J. H. Sun, J Power Sources, 174 (2007) 335-341.

18. H. F. Xiang, H. Y. Xu, Z. Z. Wang, C. H. Chen, J. Power Sources, 173 (2007) 562-564.

19.. J. K. Feng, X. P. Ai, Y. L. Cao, H. X. Yang, J. Power Sources, 177 (2008) 194-198.

20. N. Choi, K. Yew, K. Lee, M. Sung, H. Kim, S. Kim, J. Power Sources, 161 (2006) 1254-1259.

21. N. Choi, K. Yew, H. Kim, S. Kim,W. Choi, J. Power Sources, 172 (2007) 404-409.

22. M.Xu, L.Zhou, L. Hao, L. Xing, W. Li, B.L.Lucht, J. Power Sources, 196, (2011) 6794-6801.

	Electrolyte	Composition
1	**Standard**	1.2M LiPF6 EC/EMC (3:7) vol.%
2	**LiBOB**	1.0M (95% $LiPF_6$ + 5% LiBOB) EC/EMC (3:7) vol.%
3	**TPP**	1.0M $LiPF_6$ EC/EMC/TPP (3:6:1) wt.%
4	**TPP and LiBOB**	1.0M (95% $LiPF_6$ + 5% LiBOB) EC/EMC/TPP (3:6:1) wt.%
5	**DMMP**	1.0M $LiPF_6$ EC/EMC/DMMP (3:6:1) wt.%
6	**DMMP and LiBOB**	1.0M (95% $LiPF_6$ + 5% LiBOB) EC/EMC/DMMP (3:6:1) wt.%

Table 3-1. Electrolyte blend compositions

Electrolyte	1st Cycle Efficiency (%)	Capacity Retention 5th Cycle (%)	Capacity Retention 55th Cycle (%)
Std. Binary - 1.2M LiPF6 EC/EMC (3:7) vol.%	69	97	59
Std.w/ 5% LiBOB - 1.0M (95% $LiPF_6$ + 5% LiBOB) EC/EMC (3:7) vol.%	46	91	87
10% TPP - 1.0M $LiPF_6$ EC/EMC/TPP (3:6:1) wt.%	62	94	71
10% TPP w/ 5% LiBOB - 1.0M (95% $LiPF_6$ + 5% LiBOB) EC/EMC/TPP (3:6:1) wt.%	64	90	83
10% DMMP - 1.0M $LiPF_6$ EC/EMC/DMMP (3:6:1) wt.%	60	95	51
10% DMMP w/ 5% LiBOB - 1.0M (95% $LiPF_6$ + 5% LiBOB) EC/EMC/DMMP (3:6:1) wt.%	51	94	87

Table 3-2. 1st Cycle Efficiency & Capacity Retention at 5^{th} and 55^{th} cycles for cells using FR electrolyte with/without LiBOB.

	C 1s (%)	F 1s (%)	O 1s (%)	Si 2p (%)	P 2p (%)	B 1s (%)
Fresh Si Anode	25	-	52	23	-	-
Std. - 1.2M LiPF6 EC/EMC (3:7) vol.%	40	20	39	1	-	-
Std.w/ 5% LiBOB - 1.0M (95% $LiPF_6$ + 5% LiBOB) EC/EMC (3:7) vol.%	40	4	48	-	-	8
10% TPP - 1.0M $LiPF_6$ EC/EMC/TPP (3:6:1) wt.%	34	24	38	-	4	-
10% DMMP - 1.0M $LiPF_6$ EC/EMC/DMMP (3:6:1) wt.%	26	31	37	2	4	-
10% TPP w/ 5% LiBOB - 1.0M (95% $LiPF_6$ + 5% LiBOB) EC/EMC/TPP (3:6:1) wt.%	38	4	50	-	1	7
10% DMMP w/ 5% LiBOB - 1.0M (95% $LiPF_6$ + 5% LiBOB) EC/EMC/DMMP (3:6:1) wt.%	36	10	46	-	2	6

Table 3-3. Elemental concentration of C, O, F, P, Li, and B on Fresh vs. cycled Si anodes using FR electrolyte with/without LiBOB after 5 cycles.

	C 1s	F1s	O 1s	Si 2p	P 2p	B 1s
Fresh Si Anode	25	-	52	23	-	-
Std. Binary - 1.2M LiPF6 EC/EMC (3:7) vol.%	29	44	23	1	3	-
Std. Binary w/5% LiBOB–1.0M $LiPF_6$ (95% LiPF6 + 5% LiBOB) EC/EMC (3:7) vol.%	42	2	51	-	1	4
10% TPP - 1.0M $LiPF_6$ EC/EMC/TPP (3:6:1) wt.%	26	34	37	-	3	-
10% DMMP - 1.0M $LiPF_6$ EC/EMC/DMMP (3:6:1) wt.%	25	40	31	2	2	-
10% TPP w/ 5% LiBOB - 1.0M (95% $LiPF_6$ + 5% LiBOB) EC/EMC/TPP (3:6:1) wt.%	41	4	49	-	1	5
10% DMMP w/ 5% LiBOB - 1.0M (95% $LiPF_6$ + 5% LiBOB) EC/EMC/DMMP (3:6:1) wt.%	34	7	42	-	1	9

Table 3-4. Elemental concentration of C, O, F, P, Li, and B on Fresh vs. cycled Si anodes using FR electrolyte with/without LiBOB after 55 cycles.

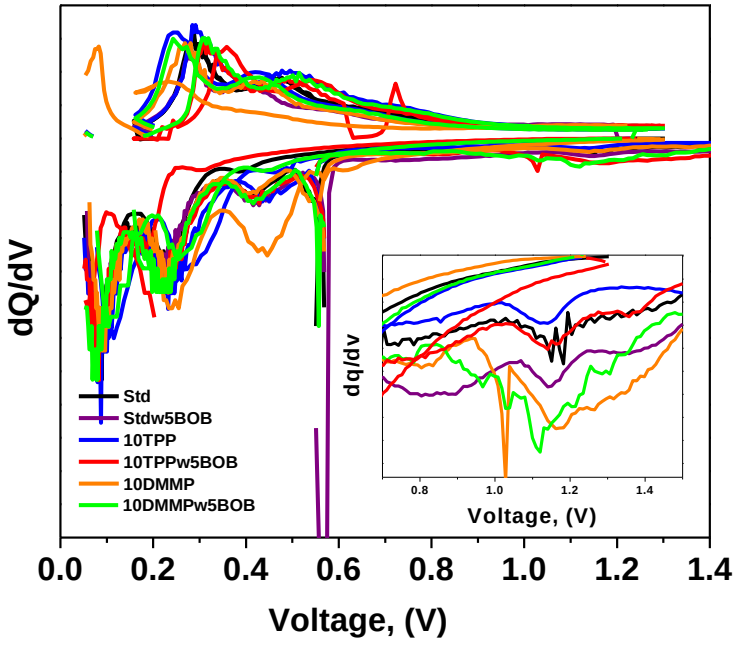

Figure 3-1. Combined dQ/dV of Std. vs. Std w/ 5% LiBOB vs. 10%TPP vs. 10%TPP w/ 5% LiBOB vs. 10%DMMP vs. 10%DMMP w/ 5% LiBOB.

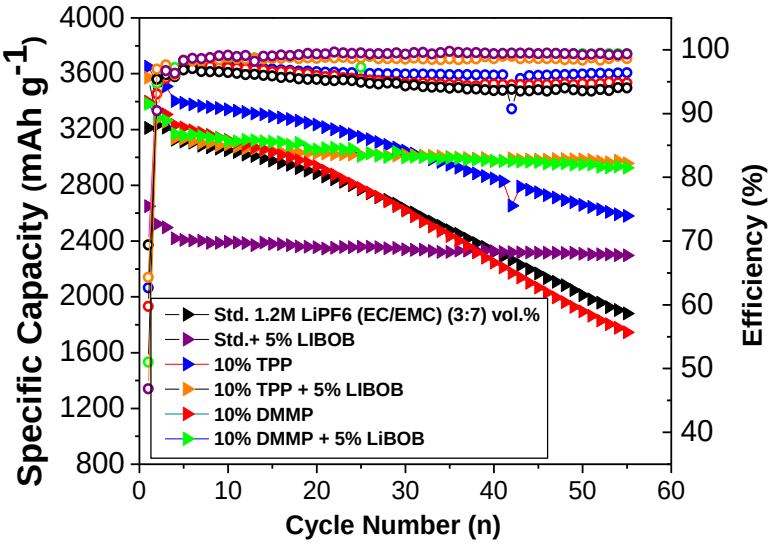

Figure 3-2. Cycling Performance of Si/Li half cells utilizing Std. 1.2M $LiPF_6$ (EC/EMC) (3:7) vol.%, Std. with 5% LiBOB, 10% TPP, 10% TPP with 5% LiBOB, 10% DMMP, 10% DMMP with 5% LiBOB.

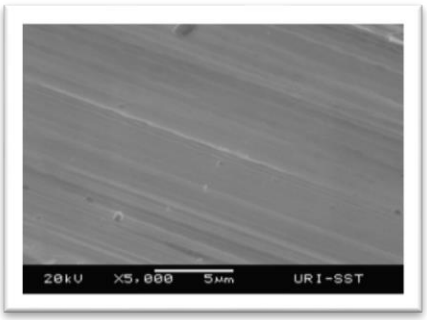

Fresh

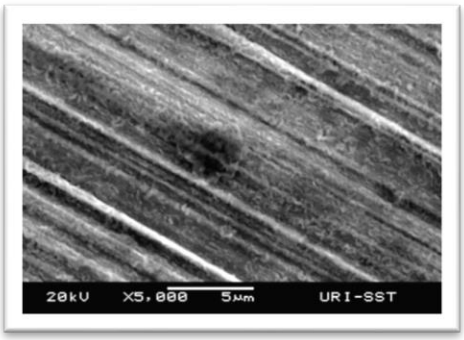

a

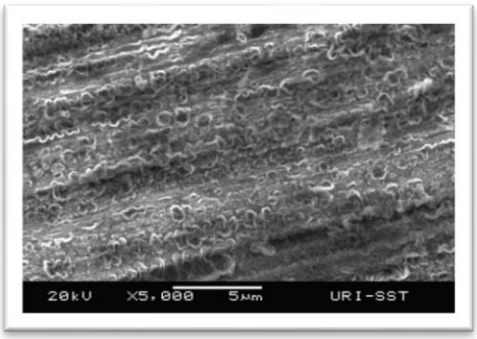

b

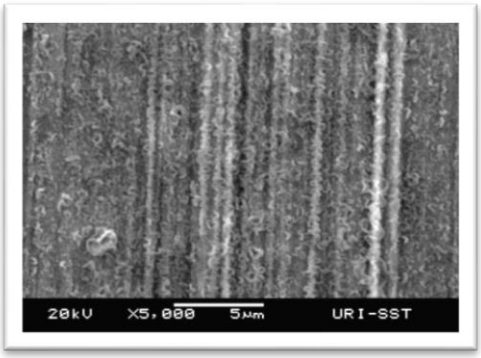

c

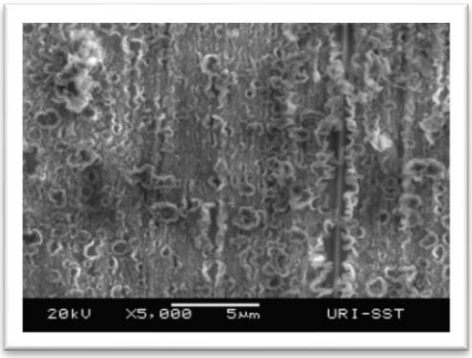

d

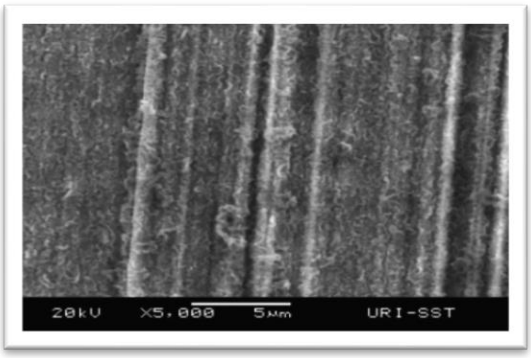

e

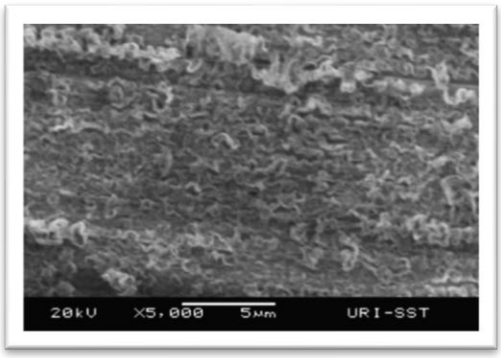

f

Figure 3-3. SEM imaging of Si anodes after 55 cycles with (a) Std. 1.2M $LiPF_6$ (EC/EMC) (3:7) vol.%, (b) Std. with 5% LiBOB, (c) 10% TPP, (d) 10% TPP with 5% LiBOB, (e) 10% DMMP, (f) 10% DMMP with 5% LiBOB.

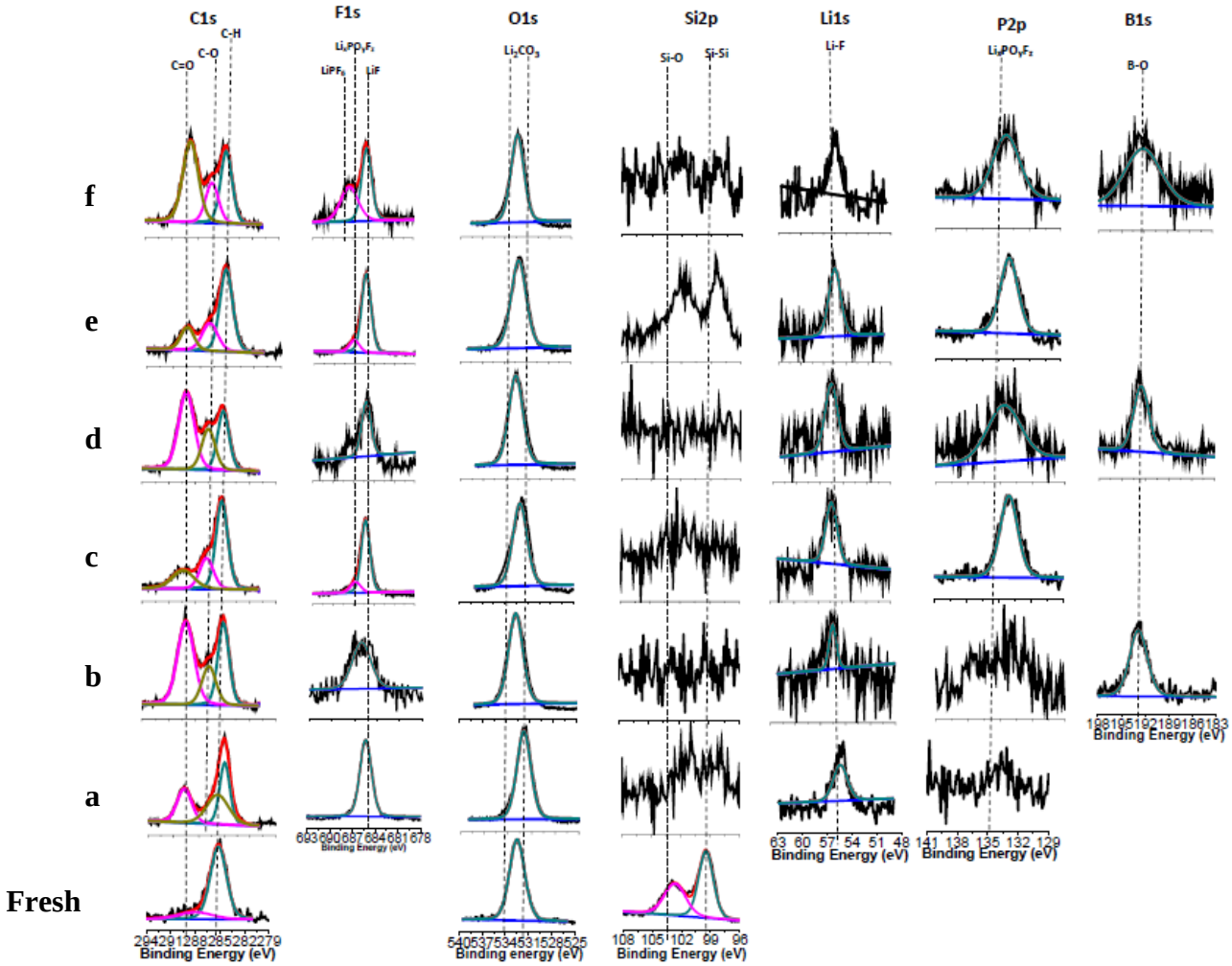

Figure 3-4: XPS Spectra of Si anodes after 5 cycles with (a) Std.,(b) Std. + 5% LiBOB; (c)10% TPP, (d) 10% TPP + 5% LiBOB; (e) 10% DMMP; (f) 10% DMMP + 5% LiBOB.

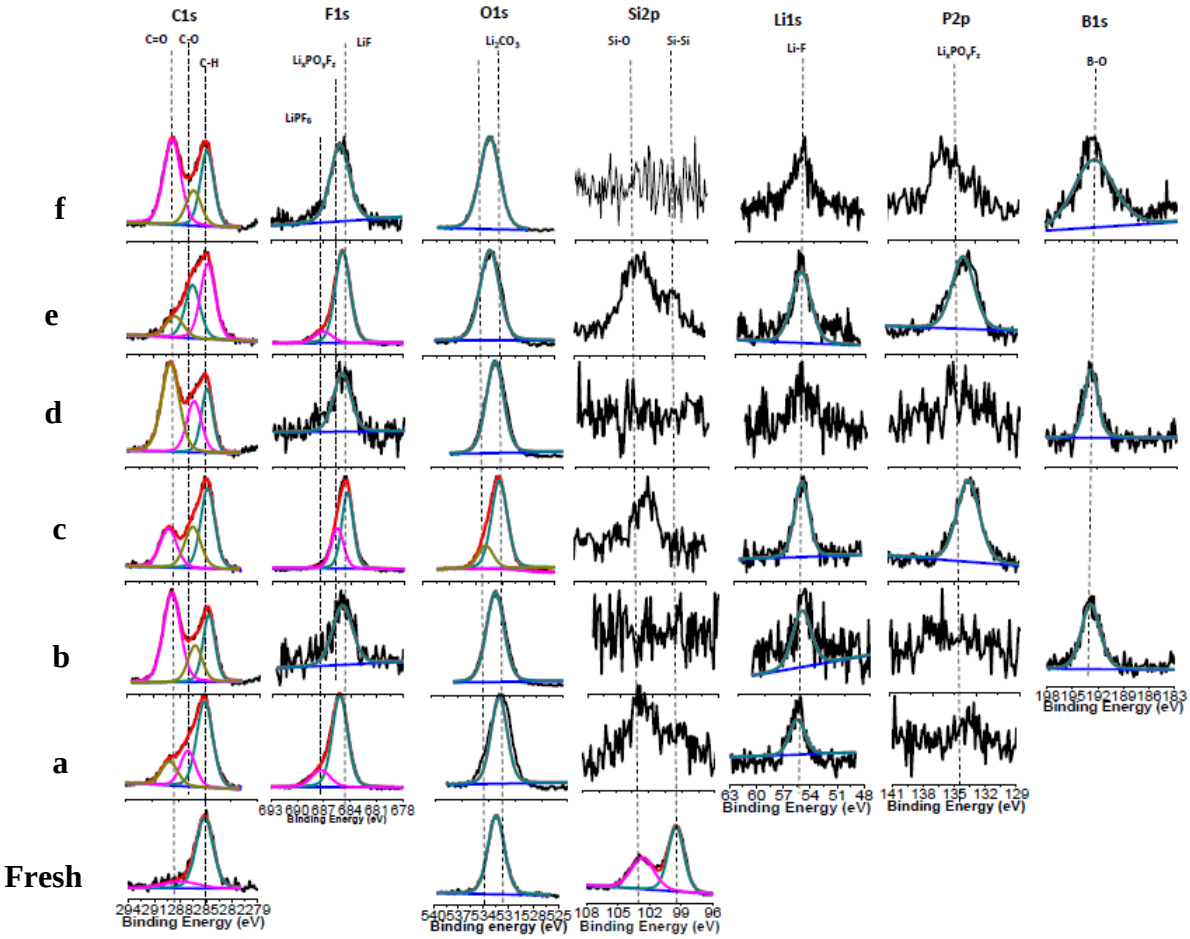

Figure 3-5: XPS Spectra of Si anodes after 55 cycles. (a) Std., (b) Std. + 5% LiBOB, (c) 10% TPP, (d) 10% TPP + 5% LiBOB, (e) 10% DMMP, (f) 10% DMMP + 5% LiBOB.

Chapter 4

Flame Retardant Cosolvent Incorporation into Lithium-Ion Coin Cells with Si Nanoparticle Anodes

Ronald P. Dunn, Cao Cuong Nguyen, Brett L. Lucht

Department of Chemistry, University of Rhode Island,

Kingston, Rhode Island 02881, USA

The following is in preparation for submission to the *Journal of Power Sources*, and is presented here in manuscript format.

Abstract

The natural flammability characteristics of standard Li-Ion battery electrolyte and associated safety concerns have led to research centered on the incorporation of Flame retardant (FR) cosolvents or additives. There has also been parallel interest in the development of high capacity electrodes to address the call for Li-Ion batteries with greater energy density. The electrochemical stability of Si-nanoparticle /Li half cells using standard binary $LiPF_6$/ethylene carbonate (EC)/Ethyl methyl carbonate (EMC) electrolytes with incorporated Triphenyl phosphate (TPP) and Dimethyl methylphosphonate (DMMP) was evaluated via cell cycling. Anode SEI film stabilizing fluoroethylene carbonate (FEC) was also utilized so as to stabilize performance. The incorporation of TPP and DMMP into standard electrolyte together with FEC additive results in comparable improvements in capacity retention to that observed in cells with standard electrolyte and FEC when cycling in Si-nanoparticle anode half cells.

Introduction

Li-ion batteries are now the energy storage technology of choice for commercial electronics including laptop computers and smartphones. In addition, Li-ion battery packs are now being introduced to high energy applications such as the automotive and aerospace arenas. Li-ion batteries offer higher volumetric and gravimetric energy densities versus NiMH, NiZn and Lead-Acid battery systems which as a result yield a light weight and longer running energy storage alternative. [1-2]

The introduction of Li-ion batteries to systems with high energy requirements such as electric vehicles (EV's) and aerospace platforms has prompted the research community to study Si for practical use as an anode material. Si offers substantially higher theoretical specific capacity (3579 mAh/g) compared to Graphite anodes (372 mAh/g).[3,4] Large platform implementation of Li-ion battery packs also brings with it increased concerns towards safety issues that are inherent to Li-ion cells. Standard Li-ion battery electrolyte is composed of naturally flammable binary or ternary mixtures of Ethylene carbonate (EC) with Ethyl methyl carbonate (EMC), Diethyl carbonate (DEC), or Dimethyl carbonate (DMC). The possibility of cell thermal runaway via heat buildup within the cell, and/or cell over-charge/over-discharge is thus a constant hazard. [5,6]

The safety concerns associated with Li-ion cell thermal runway have led to efforts by various research groups to investigate the development and practical incorporation of Flame retardant (FR) cosolvents/additives. Organophosphate containing compounds have been examined by several groups due to their natural flame suppressing properties [7-8] including Trimethyl phosphate (TMP) [9], 4-Isopropyl Phenyl Diphenyl Phosphate (IPPP) [10], Triphenyl Phosphate (TPP) [8,11-15] and Dimethyl methylphosphonate (DMMP) [7, 16-18] Significant reductions in the flammability of standard electrolyte have be attained through the use of Triphenyl phosphate (TPP) and Dimethyl methylphosphonate (DMMP) incorporation with comparable cycling performance to standard electrolyte. [8,9, 11-18]

Anode SEI film stability issues with the incorporation of some FR additives have been encountered including poor capacity retention and poor low temperature

performance. Various groups have as a result investigated the benefits offered through the parallel addition of SEI film forming additives including vinylene carbonate (VC), and lithium bis(oxalato)borate (LiBOB). [7,8, 12-14, 19]

The practical commercial implementation of Si anodes has been wrought with challenges relating to the enormous volume changes (3-4 fold) which take place during cycling.[3] The enormous volume changes which take place with repeated cell charging and discharging results in substantial mechanical stress both upon the Si-current collector interface as well as internal stresses to the Si alloy structure. This stress can lead to loss of electrical contact between the current collector and bulk Si active material as well as the loss of electrical contact between the individual Si particles. [3,20]

Continual breakdown and subsequent reformation of the protective solid electrolyte interphase (SEI) layer occurs as a result of the massive surface area changes during Si anode cycling. This continuous SEI formation process leads to large irreversible initial capacity loss, poor cycling stability, and shorter overall cell life. Many research groups have centered efforts on decreasing Si particle size via the use of thin-films Si anodes as well as through the use of Si-active and Si-inactive composite materials so as to moderate/alleviate the effects of Si expansion. [4,20-21] The use of inactive conductive carbon black in Si composite materials has received interest due to their cushioning towards the active Si volume expansion as well as improving the overall electrical conductivity of the active material structure. [3,21]

The development of a suitable binder for Si anodes has also received attention as its role predicated on the maintaining electrical conductivity throughout the electrode. Standard poly(vinylidene fluoride) (PVDF) binder is known not to be effective towards accommodating the internal stresses inherent to Si volume expansion during repeated cycling. Thus, several groups have studied the use of alternative binders to further aid in mitigation of the internal stresses associated with Si volume expansion. Both sodium carboxymethyl cellulose (Na-CMC) and poly(acrylic acid) (PAA) have garnered interest due to their superior adhesion qualities. [22,23] In addition, various groups have reported the cycling benefits offered through the use of fluoroethylene carbonate (FEC) as an additive for Si anodes. [4, 23-25]

The focus of many investigations has been FR cosolvent/additive incorporation into standard Li-ion electrolyte in an effort to enhance safety through reduced flammability without sacrificing electrochemical performance. Simultaneously, there has been a push towards the development of Si composite anodes so as to produce a practical high capacity anode alternative for high power Li-ion battery applications. This investigation centers on the electrochemical performance of Si-nanoparticle anodes cycled with TPP and DMMP containing electrolytes combined with SEI film stabilizing FEC additive.

Experimental

Battery grade ethylene carbonate (EC), ethyl methyl carbonate (EMC), and dimethyl carbonate (DMC), and lithium hexafluorophosphate ($LiPF_6$) were obtained from BASF. Standard 1.2 M $LiPF_6$ (EC/EMC) 3:7 (vol.%) electrolyte was obtained from BASF and utilized without additional purification. Battery grade fluoroethylene carbonate (FEC) was also acquired from BASF. Dimethyl methyl phosphonate (DMMP) was purchased from Sigma-Aldrich and subsequently dried with sodium hydride and molecular sieves prior to purification via vacuum distillation. The purity of DMMP was confirmed via gas chromatography with mass selective detection (GC-MS). Triphenyl phosphate (TPP) was obtained from Thermo Fisher Scientific with a purity of 99%. FR electrolyte solutions with FEC were prepared with a constant concentration of EC and $LiPF_6$. FR co-solvent as well as FEC introduction corresponded with a decrease in EMC concentration.

Si electrodes were prepared using Si ≤50nm nanopowder purchased from Alfa Aesar. PAA (Avg. $M_w \approx 470\ 000$) was obtained from Sigma-Aldrich. Na-CMC (Avg. $M_w \approx 700\ 000$) and Carbon black powder (Super C-65) were also obtained from Timcal. The Silicon, Super C, and a 1.5wt% of PAA-CMC (50:50, w/w) solution in water were mixed in an Agate mortar with pestle for 2h &30 mins. During grinding, ≈3 ml of water was added to control the viscosity. The resultant slurry was spread on 15 µm of Cu foil with a 110 µm doctor blade. The electrode was left to dry in the air at room temperature for 2 hr and then dried under vacuum at room temperature overnight. After drying overnight, the electrodes have a thickness of ≈12micron. The electrodes were then punched to a disk shape with a 12.7 mm diameter. The punched

electrodes were dried again in a vacuum oven at 110°C for 12 hrs. All electrodes contained approximately 60% Si, 20% of Carbon black (Super C), and 20% of PAA-CMC binder at a ratio of 1:1.

Cells were cycled at constant-current charge and constant voltage between 1.5 V and 0.05 V using an Arbin BT4010 battery cycler at 60 °F (16 °C). The coin cell cycling protocol followed a schedule consisting of a C/5 current rate for 50 cycles. Coulombic efficiency is defined as the ratio of discharge capacity of the cell to charge capacity at a particular cycle. Capacity retention is defined as the ratio of discharge capacity at a particular cycle to the recorded maximum discharge capacity.

Results & Discussion

The cycling performance ramifications of TPP and DMMP FR cosolvent incorporation into standard electrolyte was studied in Si-nanoparticle/Li half cells and is shown along with coulombic efficiency in Fig.1. The 1st cycle coulombic efficiencies of cells after 50 cycles are shown in Table 2.

Cells cycled with standard electrolyte show an initial (1^{st}) cycle efficiency of (88%) and a maximum capacity of ($\geq$ 2800 mAh/g) prior to substantial fade. The cell efficiency is low during the first few cycles (65 - 85 %) but is improved to 95-96 % with subsequent cycling. Cells cycled with standard electrolyte with FEC as well as those cycled with DMMP and FEC both show similar 1^{st} cycle efficiency, lower maximum capacity ($\geq$ 2600 mAh/g), and substantially improved capacity retention (74% and 66% after 50 cycles) with nominal cycling efficiencies of (95-97%) and (97-

98%) respectively. Cells cycled with electrolyte containing TPP and FEC have the lowest 1st cycle efficiency (74-75%), but highest maximum capacity (≥3000 mAh/g). In addition, cells with TPP and FEC have good cycling efficiency, 97%, and capacity retention, 63 %, after 50 cycles. Some of the initial efficiency differences can be attributed to the Li metal counter electrode..

Overall, the results indicate that cycling of Si-nanoparticle electrodes with electrolytes containing FR cosolvent and FEC have comparable performance to cells cycled using standard electrolyte with FEC.

Conclusions

The cycling performance of Si-nanoparticle anodes with electrolytes containing FR co-solvents TPP and DMMP and SEI stabilizing co-solvent FEC have been investigated. Si/Li half cells cycled with standard electrolyte have substantial capacity fade over the first 50 cycles, 39 % capacity retention. The use of FEC as a SEI film stabilizer significantly improves the cycling stability. A capacity retention of 74% is observed after 50 cycles. Cells cycled with DMMP and FEC containing electrolyte show comparable capacity retentions, 66%, and first cycle efficiency, 64 %. Cells cycled with TPP and FEC containing electrolyte also have similar capacity retention, 63%, and greater maximum capacity (3000 mAh/g). In conclusion, incorporation of FR co-solvents TPP and DMMP into Si-nanoparticle electrodes coupled with the use of SEI stabilizing FEC can provide comparable cycling performances to standard electrolytes at levels known to offer FR benefit.

Acknowledgement

This research project was funded by the NASA EPSCoR program.

References

1 D. Linden., Handbook of Batteries, fourth ed., McGraw-Hill Professional, New York, 2010.

2. K. Xu, Chem. Rev. 104 (2004) 4303.

3. U. Kasavajjula, C. Wang, A.J. Appleby, J. Power Sources 163 (2007) 1003.

4. S. Dalavi, P.R. Guduru, B.L. Lucht, J. Electrochem. Soc. 159 (2012) A642.

5. M. C. Smart, B. V. Ratnakumar, S. Surampudi, J. Electrochem. Soc. 146 (1999) 486-492.

6. K. Xu, M. S. Ding, S. Zhang, J. L. Allen, T. R. Jow, J. Electrochem. Soc. 149 (2002) A622-A628.

7. S. Dalavi, B.L.Lucht, B. Ravdel, M. Xu, L.Zhou, J. Electrochem. Soc. 157, (2010) A1113-A1120.

8. R.P.Dunn, J. Kafle, F.C.Krause, C.Hwang, B.V.Ratnakumar, M.C.Smart, B.L.Lucht, J. Electrochem. Soc. 159, (2012) A2100-A2108.

9. X. Wang, E. Yasukawa, S. Kasuya, *J. Electrochem. Soc.*, **148,** A1058 (2001)

10. Q.Wang, J. Sun, X.Yao, C. Chen, Electromchem, Solid State Lett. 8 (9) (2005) A467-A470.

11. E. G. Shim, T. H. Nam, J. G. Kim, H. S. Kim, and S. I. Moon, J. Power Sources.172 (2007) 919-924.

12. K. A. Smith, M. C. Smart, G. K. S. Prakash, and B. V. Ratnakumar, ECS Trans. 16(35) (2009) 33-41.

13. M. C. Smart, F. C. Krause, C. Hwang, W. C. West, J. Soler, G. K. S. Prakash, and B. V. Ratnakumar, ECS Trans. **35**(13) (2011) 1-11.

14. E. G. Shim, T. H. Nam, J. G. Kim, H. S. Kim, S. I. Moon, J. Power Sources, 172 (2007) 901-907.

15. Y. E. Hyung, D. R. Vissers, and K. Amine, J. Power Sources, 119-121 (2003) 383-387.

16. H. F. Xiang, Q. Y. Jin, C. H. Chen, X. W. Ge, S. Guo, J. H. Sun, J Power Sources,174 (2007) 335-341.

17. H. F. Xiang, H. Y. Xu, Z. Z. Wang, C. H. Chen, J. Power Sources, 173 (2007) 562-564.

18. J. K. Feng, X. P. Ai, Y. L. Cao, H. X. Yang, J. Power Sources, 177 (2008) 194-198.

19. L. Chen, K. Wang, X. Xie, J. Xie, J. Power Sources, 174 (2007) 538-543.

20. M.N. Obrovac, L.J. Krause, J. Electrochem. Soc. 154. (2007) A103-A108.

21. W.R. Liu, Z.Z Guo, W.S.Young, D.T. Shieh, H.C.Wu, M.H. Yang, N.L. Wu, J. Power Sources, 140 (2005) 139-144.

22. A.Magasinski, B. Zdyrko, I. Kovalenko, B. Hertzberg, R. Burtovyy, C. F. Huebner, T. F. Fuller, I. Luzinov, and G. Yushin, ACS Applied Materials & Interfaces 2 (11) (2010) 3004-3010.

23. H. Buqa, M. Holzapfel, F. Krumeich, C. Veit, P. Novak, J. Power

Sources 161 (2006) 617–622.

24. H. Nakai, T. Kubota, A. Kita, A. Kawashima, J. Electrochem. Soc., 158, (2011) A798-A801.

25. V. Etacheri, O. Haik, Y. Goffer, G. A. Roberts, I. C. Stefan, R. Fasching, D.Aurbach, Langmuir, 28 (1),(2012) 965-976.

	Electrolyte	Composition
1	**Standard**	1.0M LiPF6 EC/EMC (3:7) vol.%
2	**10% FEC**	1.0M $LiPF_6$ EC/EMC/FEC (3:6:1) wt.%
3	**10% TPP w/ 10% FEC**	1.0M $LiPF_6$ EC/EMC/TPP/FEC (3:5:1:1) wt.%
4	**10% DMMP w/ 10% FEC**	1.0M $LiPF_6$ EC/EMC/DMMP/FEC (3:5:1:1) wt.%

Table 4-1. Electrolyte blend compositions

Electrolyte	Initial (1st Cycle) Efficiency	Capacity Retention-50th Cycle
Std.	88	39
Std.w/ 10% FEC	83	74
10% TPP w/ 10% FEC	74	63
10% DMMP w/ 10% FEC	88	66

Table 4-2. 1st Cycle Efficiency & Capacity Retention after 50 cycles for cells using FR electrolyte with FEC additive

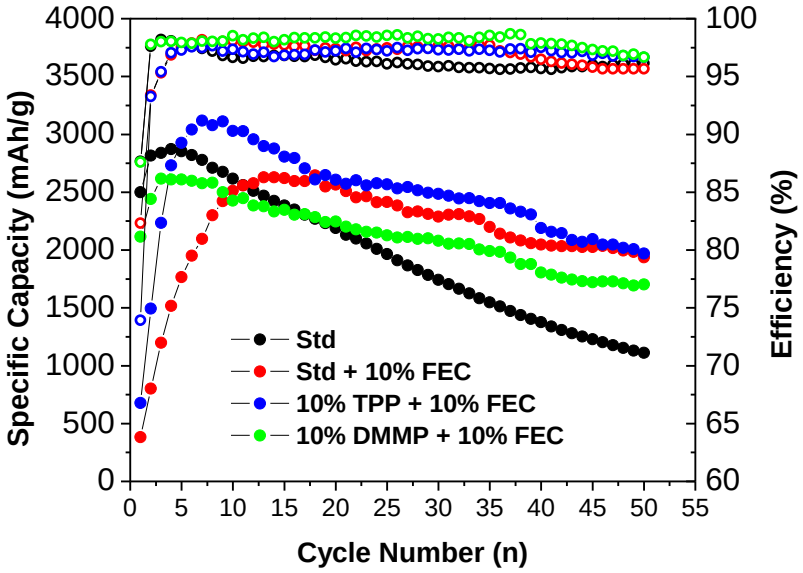

Figure 4- 1. Cycling Performance of Si/Li half cells utilizing Std. 1.2M $LiPF_6$ (EC/EMC) (3:7) vol.%, Std. with 10% FEC, 10% TPP with 10% FEC, 10% DMMP with 10%FEC.

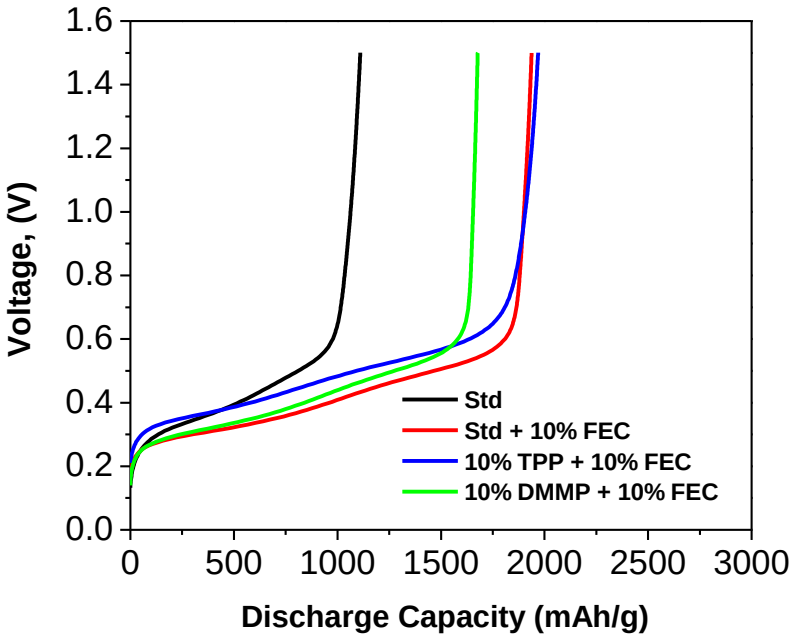

Figure 4- 2. Discharge profiles for Si-nanoparticle/Li cells on the 50th cycle with and without FR+FEC electrolyte.